Appendix 3B-3: Approaches to Modeling Sulfate Reduction and Methylmercury Production in the Everglades

Cynthia Gilmour[1], Eric Roden[2] and Reed Harris[3]
(Final Report, May 2007)

Note: For reader convenience, Appendix 3B-3 is being reproduced verbatim and has not been revised through peer review or by the SFER production staff. This appendix was provided by the above-listed authors with several affiliations under Contract # CP060613, and does not necessarily reflect the views or opinions of the South Florida Water Management District and the Florida Department of Environmental Protection.

[1] Smithsonian Environmental Research Center, Edgewater, MD

[2] University of Wisconsin, Department of Geology and Geophysics, Madison, WI

[3] Tetra Tech, Inc., Ontario, Canada

FINAL REPORT

APPROACHES TO MODELING SULFATE REDUCTION AND METHYLMERCURY PRODUCTION IN THE EVERGLADES

Tasks 5 and 6

MAP for RECOVER Section 3.6.4.4

Supporting Research for South Florida Mercury Bioaccumulation

May, 2007

Cynthia Gilmour
Smithsonian Environmental Research Center
647 Contees Wharf Road
Edgewater, Maryland 21037
443-482-2498
gilmourc@si.edu

Eric Roden
University of Wisconsin
Dept. of Geology and Geophysics
1215 W. Dayton St.
Madison, WI
608-890-0724
eroden@geology.wisc.edu

Reed Harris
Tetra Tech Inc.
180 Forestwood Drive
Oakville, Ontario
Canada L6J4E6
tel: 905 339 0763
fax: 905 339 0764
rharris6@cogeco.ca

SUMMARY

Existing mercury cycling models do not adequately capture the complex interactions between methylmercury (MeHg) production and the sulfur cycle. In the Everglades, and in most other ecosystems, the sulfur cycle is a primary control on net MeHg production and bioaccumulation (along with inorganic Hg inputs and organic matter availability). In this report, two models are used to try and capture the biogeochemical relationships between the Hg and S cycles, and to apply them to the Everglades.

This report comprises the modeling sections of a larger study on sulfur, and its relationships to mercury, in the Everglades. The report is the work product for Tasks 5 and 6 of MAP for RECOVER Section 3.6.4.4, "Supporting Research for South Florida Mercury Bioaccumulation." The overall objective of that study has been to provide an initial assessment of sulfur in the Everglades Protection Area, including an evaluation of sulfur distributions, trends and potential sources; a report on potential sulfur minimization and mitigation strategies; and development of mechanistic models for methylmercury production in the Everglades that better incorporate sulfur cycling. The initial findings from tasks 1-3 were reported 2007 SFER Appendix 3B-3, and the final work production for tasks 1-4 is in May 2007 report, "An Initial Assessment of Sulfur Distribution, Trends, Sources and Potential Mitigation in the Everglades."

Specific modeling objectives were 1) to develop a diagenetic transport-reaction model that is capable of predicting the depth distribution of Hg methylation as a function of soil biogeochemistry, and 2) to explore how that model could be used to improve the ability of the Everglades Mercury Cycling Model (E-MCM) to predict responses to changing sulfate concentrations in the Everglades. E-MCM is an existing model of mercury cycling and bioaccumulation in Everglades marshes (E-MCM, Tetra Tech 1999). It includes algorithms to represent microbial methylation of mercury, but it is unresolved how to best link methylation in E-MCM to sulfur cycling. Once developed, one or both models would then be available to help predict how ecosystem restoration and potentially sulfate management practices could affect MeHg production and bioaccumulation in the Everglades Protection Area.

Diagenetic models are numerical simulations of the post-burial decomposition of organic matter via a sequence of microbial fermentative and respiratory processes. In these models, microbial organic matter oxidation is driven by the vertical flux of oxidants (ie. oxygen, nitrate, sulfate) into sediments and soils. The models link microbial activity to sediment chemistry. The specific goal of this study was construct a model that is capable of predicting the depth distribution of Hg methylation in Everglades soils across a range of surface water sulfate concentrations. To do so, simulations for Hg speciation and microbial methylmercury production and degradation were added to a general diagenetic model strucuture (e.g. Boudreau et al. 1998).

The model developed for this study depicts major diagenetic processes in the vertical dimension (i.e. a 1-dimensional transport-reaction model), including diffusion and particle mixing; major microbial terminal electron accepting processes (ie, oxygen, iron, nitrate and sulfate respiration); equilibrium speciation of dissolved ferrous Fe, Hg, DIC, sulfide and Hg; kinetically-controlled sorption of ferrous iron, inorganic Hg, and methyl-Hg to the sediment solid-phase; and kinetically-controlled precipitation of FeS and HgS.

The diagenetic Hg and S cycling model developed for this study was applied to several sites within Storm Treatment Area (STA) 3/4 (Cells 1-3), Water Conservation Area (WCA) 2A (sites

U3 and F1), and WCA 3A (site 3A15), using detailed biogeochemical field data from the ACME study. In addition, the model was used to generate input values for E-MCM simulations of the response of site 3A15 to decreases in sulfate input over the last ca. 10 years (1995-2005).

The diagenetic model was first applied to sites U3 and F1 in WCA 2A, both high sulfate sites. Adjustable variables were scaled as need to fit the observed sulfate and dissolved Hg data. The results of these simulations were quite promising, in that it was possible to obtain better than order-of-magnitude fits of sulfate reduction rates, dissolved inorganic Hg concentrations and total MeHg concentrations. After initial calibration using data from the WCA 2A sites, the diagenetic model was applied to an AMCE biogeochemical data set for soils in multiple cells of STA 3/4. Again, the model was able to accurately reproduce the observed aqueous and solid-phase Hg data, and total MeHg concentrations after adjustment of the scalable variables to match sulfate and dissolved Hg profiles.

The final application of the diagenetic model was to site 3A15 in WCA 3A, which has been studied for over a decade through the ACME study and other programs. Surface water sulfate concentrations have dropped during that decade, along with MeHg levels in water, sediments and fish. The diagenetic model was calibrated to fit observed downcore data from 1996 through 1998, then used to predict depth-integrated sulfate reduction rates and MeHg concentrations over the full decade. Model outputs accurately predicted the concomitant declines in sulfate reduction rate and MeHg production at this site over time, providing mechanistic support for the hypothesis that sulfate declines are driving at least part of the observed decline in MeHg at this site.

The Everglades Cycling model is a mechanistic simulation model that uses a mass balance approach to predict time-dependent concentrations for three forms of mercury: inorganic Hg(II), methylmercury and elemental mercury. E-MCM was originally calibrated to site WCA 3A-15 as part of a pilot mercury TMDL (Tetra Tech 2003). That calibration did not include any dependency of methylation on sulfate. However, the model does include an optional algorithm that allows methylation rates to be linearly dependant on sulfate concentration. Here, previous calibrations of E-MCM for WCA 3A-15 were extended by comparing results with the following approaches to methylation: 1) methylation is not affected by sulfate; 2) methylation is related to observed sulfate concentrations by making methylation rate a linear function of sulfate concentration and 3) methylation is related to sulfate reduction rates. In the latter case, sulfate reduction rates were input to E-MCM from the diagenetic model. The time period modeled was 1995-2003.

The calibration of E-MCM to surface water and biota MeHg concentrations at WCA 3A-15 improved when the model included the linear dependency of methylation rate on surface water sulfate concentration, or when the model based methylation rates on sulfate reduction rates input from the diagenetic model. The current model calibration includes a hindcast of Hg deposition rates and surface water sulfate reductions that predicted much high levels of both prior to the current simulation period. Therefore, the model's predicts declining surface water MeHg concentrations with or without assigning a sulfate dependency for methylation. However, the extent of decline was greater with a sulfate dependency, and better fit the observations. Further analysis is needed of the relative contributions of changes in sulfate, mercury loading, chloride, DOC and other factors both before 1995 and during the simulation period to the observed decline in fish mercury concentrations.

Both the diagenetic model and the sulfate-dependant versions of the E-MCM model were able to reproduce the decline in MeHg concentrations at 3A15 over the 1995-2003 period. The

diagenetic model accomplishes this mainly through equations based on first principals. These results are consistent with the hypothesis that sulfate reduction affects net methylation rates in Everglades marshes. For site 3A-15 E-MCM was able to accurately predict MeHg by making methylation dependant on sulfate concentration. However, another goal of this modeling work is to create models can reproduce MeHg concentrations across the large sulfate and sulfide gradients found in the Everglades; 3A15 is a low sulfate site where sulfide concentrations have been low throughout the study period. In order to predict MeHg concentrations at high sulfide sites, both models required empirically-fit routines for either Hg speciation and/or methylation routines, suggesting that our current understanding of Hg complexation chemistry is insufficient to model from first principals. This is consistent with the rapidly evolving literature on Hg-S-organic matter complexation chemistry. Empirical fits to existing data can be used to apply these models now to higher sulfide sites, however, more basic information on Hg-S and Hg-OM complexation under anaerobic conditions will be needed to produce first-principles models that can be broadly applied to areas for which little field information is available.

In summary, a diagenetic, model that relates Hg methylation to microbial sulfate reduction rate was able to accurately reproduce MeHg concentrations at a number of chemically different sites in the EPA. The fit of the model to the time series of declining sulfate and MeHg at site 3A15 supports the hypothesis that sulfate is a primary driver of methylation at that site, and that reduction in Everglades surface water sulfate concentrations will help mitigate MeHg production across the EPA. Further, the E-MCM was also able to reproduce this time series when methylation was made dependant on either sulfate concentrations or sulfate reduction rate. These models could now be applied to predict the distribution of MeHg across the EPA under changing sulfate loading scenarios.

TABLE OF CONTENTS

INTRODUCTION

Background - Relationships between the sulfur and mercury cycles

In order for Hg loads to ecosystems to result in MeHg in biota, inorganic Hg must be converted into MeHg. An ecosystem's sensitivity to Hg loading is defined as the ability of that ecosystem to transform inorganic Hg load into MeHg in biota (Munthe et al. 2007). Microbial methylation of Hg within ecosystems is the principal mechanism for MeHg formation (Benoit et al. 2003; Munthe et al. 2007), and dissimilatory sulfate-reducing bacteria (SRB) are thought to be the primary mediators of methylation (Compeau and Bartha 1985, Gilmour et al.1992; King et al. 2000, 2001; Benoit et al. 2003). Research over the past decade on the geochemical control of methylation has led to us to understand that the Hg cycle is intimately linked to the sulfur cycle; and that sulfate-reducing organisms are important mediators of methylation in many environments (Benoit et al. 2003).

Biological methylation of Hg was first demonstrated in the late 1960's (Jensen & Jernelov 1969). Sulfate-reducing bacteria were first identified as important Hg methylators in marine and freshwater environments in the 1980's and early 1990's (e.g. Compeau & Bartha. 1985, Gilmour 1992). Their role in methylation has been confirmed in many ecosystem types through the use of specific metabolic inhibitors (King et al. 1999; Gilmour et al. 1998), the addition of sulfate to experimental systems ranging from sediment cores to wetlands to whole lakes (e.g. Gilmour et al. 1992, Urban et al. 1994, Bloom et al. 1991; Branfireun et al. 1999; Jeremiason et al. 2006), and spatially coincident measurement of sulfate reduction rate and MeHg production (e.g. Devereux et al. 1996, Krabbenhoft et al. 1998, Gilmour et al. 1998; King et al. 2000).

In-situ microbial methylation of inorganic Hg in surface soils and flocs is the dominant source of MeHg in the Everglades (Gilmour et al. 1998; Cleckner et al. 1999). Methylation is an anoxic process. Wetlands soils, aquatic sediments, and temporally saturated soils are often defined as the main locations for MeHg production within ecosystems (St. Louis et al. 1994, Krabbenhoft et al. 1995, St. Louis et al. 1996, Branfireun et al. 1996, Benoit et al. 1998, Gilmour et al. 1998, Krabbenhoft et al. 1998; Jeremiason et al. 2006)**.** Concentrations of MeHg in Everglades biota are strongly correlated with MeHg concentrations in Everglades surface soils. Therefore, models of mercury bioaccumulation in the Everglades must adequately capture the net microbial methylation process in surface soils and flocs.

Two recent reviews of the Hg methylation process (Benoit et al. 2003; Munthe et al 2007) outline the major controls on microbial methylation that must be captured in a numerical model. These are diagramed in Fig. 1. The first is the bioavailability of inorganic Hg for uptake by mercury methylating microorganisms, which is driven by the chemistry of the environment. A second component is the distribution and activity of microorganisms capable of methylation.

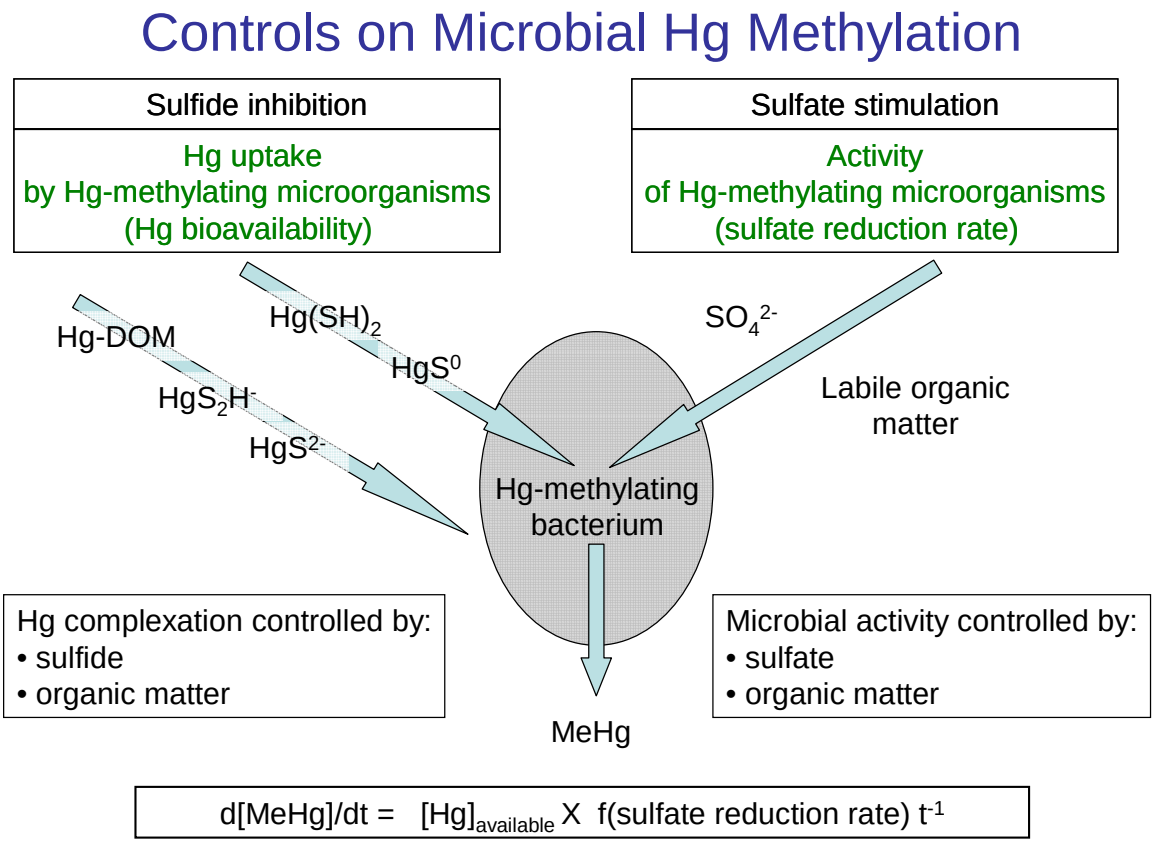

Figure 1. Conceptual diagram of the controls on microbial mercury methylation, particularly the opposing effects of sulfate and sulfide.

The production of MeHg in the Everglades is dependant on the amount of inorganic Hg available for microbial methylation and the activity of Hg-methylating organisms:

- The activity of sulfate reducing bacteria is controlled by the sulfate concentration in surface waters of the marsh, and by the overall productivity of the marsh - which provides degradable organic matter to bacteria.

- Mercury bioavailability is controlled by the complexation of dissolved Hg (Benoit et al. 1999, 2001). In the Everglades, as in many other ecosystems, sulfide and organic matter have the largest impacts on Hg complexation and bioavailability to bacteria (Benoit et al. 2003; Munthe et al. 2007).

- The balance between sulfate and sulfide controls the overall rate of MeHg production. Sulfate stimulates Hg-methylating sulfate reducing bacteria (SRB), while excess sulfide creates Hg complexes that are not bioavailable for methylation (Benoit et al. 1999; 2001).

In pure culture experiments of methylation by SRB (Benoit et al. 2000; King et al. 2000), and in field studies, the optimal concentration for methylation ranges from 10 to about 300 µM sulfate, while the optimal sulfide concentration is quite low, about 10 µM (Benoit et al. 1998; Gilmour et al. 1998). Factors such as iron and organic matter concentration that impact Hg and S complexation change these optima. Sulfate, along with pH and DOC, have been identified as parameters that relate Hg levels in fish among water bodies (Wiener et al. 2006).

In the freshwater Everglades, a very wide range of surface water sulfate concentrations across the ecosystem drives a gradient in MeHg production and bioaccumulation. The freshwater Everglades is an ecosystem that is naturally low in sulfur (Bates et al. 1998; Orem et al. 1997), impacted by sulfate inputs to the northern marshes. Fig 2 shows average surface water sulfate, sulfate reduction activity, soil pore water sulfide, and MeHg concentrations and production rates in surface soils/flocs across the main study sites of the ACME project, from 1995-1998. These data illustrate that MeHg accumulation is maximal at intermediate sulfate concentrations; where the balance between sulfate reducing activity and sulfide concentration favor higher rates of MeHg production.

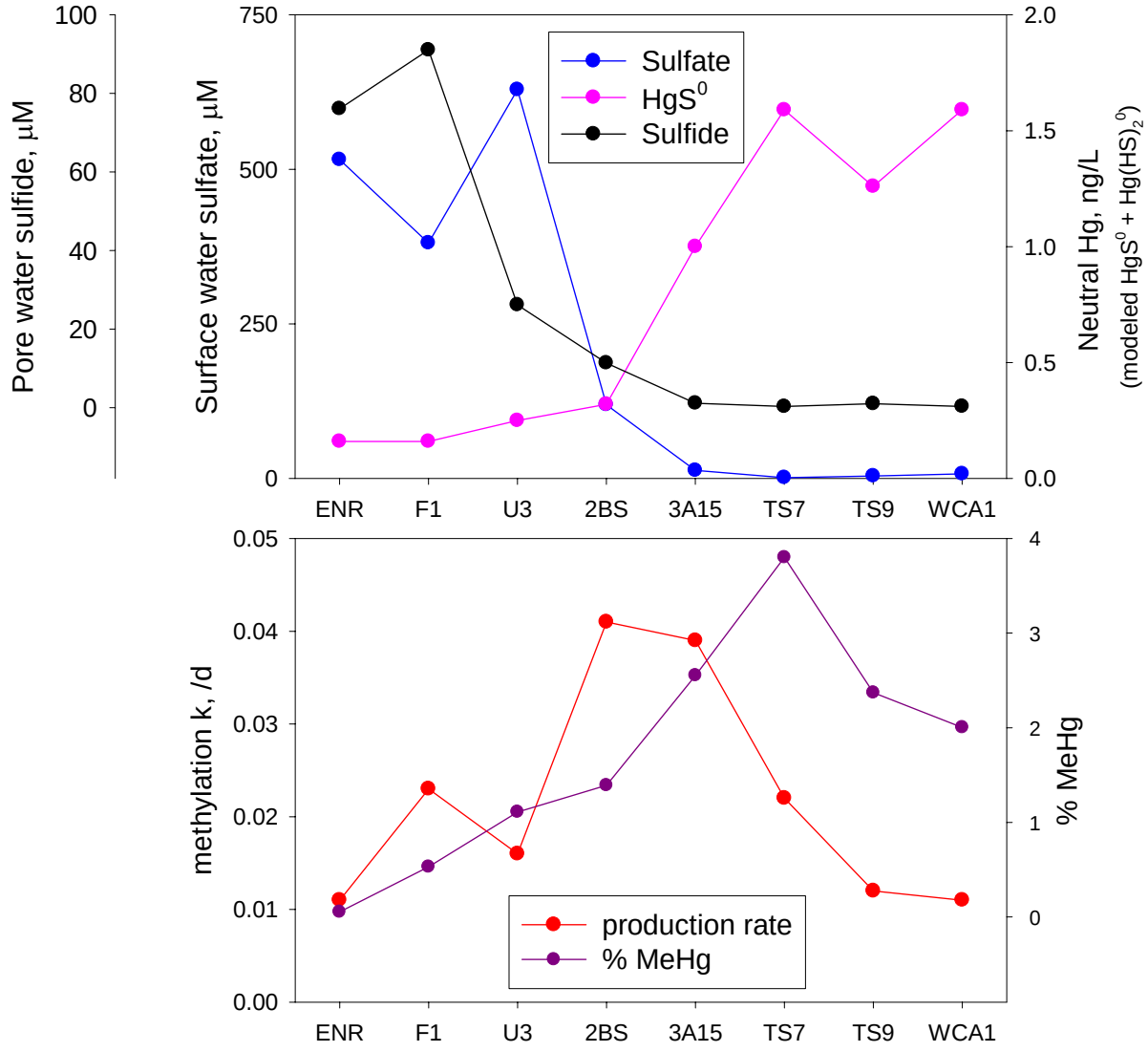

Figure 2. Measured surface water sulfate concentration, porewater sulfide concentration, percent methylmercury (%MeHg), mercury methylation rate and modeled porewater HgS^{o} in the upper 4 cm of Florida Everglades sediments at 8 ACME sites. Everglades sites are arranged from left to right by average surface water sulfate concentration (highest concentrations on the left). With the exception of the WCA 1 site, this represents a north to south transect, running from the Everglades Nutrient Removal Project (ENR) and Water Conservation Area 2A (F1, U3) in the north, through Water Conservation Areas 2B (2BS) and 3A (3A15), and to Taylor Slough in Everglades National Park (TS7, TS9) in the south. Data shown are averages from three years (1995-1998) of bi- to tri-annual sampling.

TASK 5. CONSTRUCTION OF A DIAGENETIC MODEL OF SULFATE REDUCTION AND METHYLMERCURY PRODUCTION IN THE EVERGLADES

Objective

Create a biogeochemical model of sulfur cycling in Everglades marsh soils, and use it to explore the factors governing sulfur cycling and Hg methylation. Specifically, construct a diagenetic transport-reaction model that is capable of predicting the depth distribution of Hg methylation for the Everglades and Stormwater Treatment Areas soils at different surface water sulfate concentrations.

Introduction

The coupling of Hg cycling to sediment biogeochemical processes is complex and involves issues related to Hg bioavailability (as controlled by aqueous phase speciation and aqueous/solid-phase partitioning) and the relative propensity of different principle bacterial functional groups (e.g. dissimilatory iron-reducers, sulfate-reducers, methanogens) and different genera within those groups to methylate inorganic Hg (Benoit et al., 2003). There are currently no holistic predictive models for sediment MeHg production in ecosystems. The basic goal of the modeling component of this project was to incorporate information on the biogeochemical characteristics of Everglades sediments, together with experimental and observational information on sediment Hg geochemistry and microbial transformation, into a diagenetic transport-reaction model that is capable of predicting the depth distribution of Hg methylation as a function of sediment biogeochemical zonation (see Fig. 5.1) and the relative abundance and physiological-biochemical properties of different functional groups of microorganisms. The general model developed here was applied to several sites within Storm Treatment Area (STA) 3/4 (Cells 1-3), Water Conservation Area (WCA) 2A (sites U3 and F1), and WCA 3A (site 3A15). In addition, the model was used to generate input values for E-MCM simulations of the response of site 3A15 to decreases in sulfate input over the last ca. 10 years (1995-2005).

Description of Sediment Hg Cycling Model

Overview. The sediment Hg cycling model is based on the numerical method of lines (Schiesser, 1991) implemented with the stiff ODE solver VODE (Brown et al., 1989). This approach has recently been employed successfully for modeling aquatic sediment diagenetic processes (Boudreau, 1996; Boudreau, 1997; Boudreau et al., 1998). The model depicts the following major diagenetic processes in the vertical dimension (i.e. this is a 1-dimensional transport-reaction model): (1) aqueous (diffusion) and solid-phase (random particle mixing) transport and reaction of oxygen, aqueous and sorbed ferrous iron, solid-phase ferric oxide, total dissolved inorganic carbon (DIC), sulfate, total dissolved sulfide (DS), iron monosulfide, elemental sulfur, methane, aqueous and sorbed inorganic Hg, aqueous and sorbed methyl-Hg, and cinnabar (HgS); (2) equilibrium speciation of aqueous ferrous iron, DIC, and DS (using the

MICROQL algorithm of Westall (1986)); (3) kinetically-controlled sorption of ferrous iron, inorganic Hg, and methyl-Hg to the sediment solid-phase; and (4) kinetically-controlled precipitation of FeS and HgS. A list of the primary dependent variables and a summary of the equilibrium aqueous/solid-phase equilibrium speciation system included in the model are provided in Tables 5.1 and 5.2, respectively. Standard simulations were run for a period of at least 10 years in order to achieve a dynamic steady-state. However, transient simulations are easily accommodated by the numerical method of lines approach, and were conducted to provide input to E-MCM simulations (see below).

Transport-Reaction Equations. Berner (1980) and Boudreau (1997) provide a complete derivation of the canonical forms of the mass conservation equations for solutes and solids in 1-dimensional sediment diagenetic systems. The basic transport-reaction equations for porewater solutes (C) and solid-phase species (B) employed in our model are as follows:

$$\frac{\partial \phi C}{\partial t} = \frac{\partial}{\partial x}\left(D_S \frac{\partial \phi C}{\partial x} \right) + \Sigma R$$

$$\frac{\partial (1-\phi) B}{\partial t} = \frac{\partial}{\partial x}\left((1-\phi) D_B \frac{\partial B}{\partial x} \right) + \Sigma R$$

where ϕ represents sediment porosity, D_s is the sediment diffusion coefficient for dissolved species C, D_B is the random particle mixing coefficient for solid-phase species B, and ΣR represents the sum of all kinetic and equilibrium reactions acting on the solute or solid-phase species. The sediment diffusion coefficient is related to the molecular diffusion coefficient (D_0) vis-à-vis the formation factor θ, which accounts for the influence tortuosity on rates of diffusive transport (Berner, 1980):

$$D_S = \frac{D_0}{\theta^2}$$

A standard formulation for the formation factor is

$$\theta^2 = \phi^{-p}$$

where *p* is an empirical constant that typically takes on a value between 1 and 3. In our implementation, *p* was set equal to 2, which corresponds to the most common value inferred from studies of solute diffusion in sediments (Boudreau, 1997). The observed depth distribution of sediment porosity at each study site was fit by nonlinear least-squares regression to an equation of the following form for use in the model:

$$\phi(x) = (\phi_0 - \phi_L) \times \exp(-\gamma x) + \phi_L$$

where $\phi(x)$ is the porosity at depth x, ϕ_0 is the porosity at x = 0 (i.e. at the sediment surface), ϕ_L is the porosity at the lower boundary of the modeled sediment interval (12 cm), and γ is adjustable constant. All molecular diffusion coefficients were taken from the compilation in Li and Gregory (1974), adjusted to an average temperature of 30 °C using the Stokes-Einstein relationship (Boudreau, 1997).

It is important to note that the conservation equations listed above do not include terms for advective transport, i.e. for burial fluxes of sediment solids and porewater. Burial was not considered because of the lack of well-constrained information on rates of sediment accumulation at the sites considered in our model applications. However, future implementations of the model could easily be modified to include burial fluxes.

Boundary Conditions. Careful consideration of boundary conditions is crucial for the development of sediment diagenetic models (Boudreau, 1997). Our model employs a mixture of boundary conditions chosen to allow depiction of Hg cycling coupled to sediment biogeochemical processes. Dissolved compounds such as oxygen, sulfate, DS, and DIC were assumed to have a fixed concentration in the overlying water, and to have a zero concentration gradient at lower boundary of the 12-cm deep modeled sediment layer. Solid-phase Fe and Hg compounds were assumed to have zero concentration gradients at both the upper and lower boundaries; these boundary conditions were required in order to retain Fe and Hg phases within the sediment, since the model does not explicitly include inputs of Fe and Hg through particle deposition and burial. As mentioned above, future implementations of the model could easily incorporate such flux terms, in which case the upper boundary condition for these compounds would be flux terms specified as a model input parameters. Finally, dissolved ferrous iron, dissolved inorganic Hg, and dissolved methyl-Hg were assumed to have zero concentration gradients at both the upper and lower boundaries. Here again, these conditions were required in order to retain Fe and Hg within the sediment in the absence of explicit input and burial fluxes.

Modeling the Depth Distribution of TEAPs. The depth distribution of different terminal electron accepting processes (TEAPs) was simulated based on measured (or assumed) rates of total organic decomposition (R_{CH2O}, equivalent to the rate of total CO_2 and CH_4 production) in the sediment (data available from ongoing studies in the Everglades; see Fig. 2 for an example) and a set of estimated "limiting" electron acceptor concentrations according to the "modified Monod" approach summarized in Table 5.2. In this approach, less thermodynamically favorable TEAPs become active only when the concentrations of more favorable electron acceptors fall below a prescribed limiting concentration (Boudreau, 1996; VanCappellen and Wang, 1996). The limiting concentrations for O_2, Fe(III) oxide, and SO_4^{2-} were chosen based on literature values (VanCappellen and Wang, 1995; VanCappellen and Wang, 1996) and other data

sources.

Secondary Redox Reactions. Secondary redox reactions (e.g. reduced iron and sulfur oxidation, methane oxidation) were modeled as second-order (bimolecular) rate processes, e.g. as follows for oxidation of DS by O_2:

$$R_{DS,O2} = k_{DS,O2} \times [DS] \times [O2]$$

where $k_{DS,O2}$ is a second-order rate constant (in units of (μmol mL_{aq}^{-1})$^{-1}$ d^{-1}), [DS] is the concentration of dissolved sulfide (μmol mL_{aq}^{-1}), and [O2] is the concentration of dissolved O_2 (μmol mL_{aq}^{-1}). Rate constants for the various second-order reactions were taken from the extensive compilation provided in Van Cappellen and Wang (1996) and Hunter et al. (1998). S^0 disproportionation, a potentially important S recycling process in both marine and freshwater sediments, was modeled as a first-order process which is regulated (inversely) by the concentration of dissolved sulfide (Berg et al., 2003). Inclusion of these reactions is critical for simulating the dynamic turnover of oxidized and reduced species in surface sediment transport-reaction systems (VanCappellen et al., 1993).

Hg Speciation and Biotransformation. The aqueous/solid-phase inorganic Hg speciation model described in Benoit et al. (1999) was incorporated into the diagenetic model. This model accounts for aqueous-phase equilibrium speciation reactions between Hg^{2+} and HS^-, as well as sorption reactions of Hg^{2+} with a hypothetical solid phase (ROH in Table 5.2) possessing surface sites capable of forming complexes with HS^- and Hg^{2+} ($RSHg^+$, $(RS)^2Hg$). The speciation model was modified to include an additional solid-phase capable of binding dissolved Hg^{2+} (XOH). Like the hypothetical thiol-forming solid-phase in the Benoit et al. (1999) model, the new phase was assigned a chemical activity of unity. The additional Hg sorbing phase was included to account for potential solid-phase Hg binding by mechanisms other than that depicted in the Benoit et al. (1999) model, e.g. sorption by Fe(III) oxide and/or FeS surface surfaces, or binding by non-thiol organic matter functional groups (e.g. carboxyls). The stability constant for Hg sorption to this additional phase was adjusted to the highest value (log K_f = 30) at which the concentration of dissolved Hg in the zone of dissolved HS^- accumulation was controlled by sorption to the hypothetical thiol-forming phase rather than the additional sorption phase. Precipitation of HgS(s) (like FeS(s)) was treated as a kinetically-controlled rate process dependent on the computed degree of supersaturation or undersaturation, assuming a log K_{sp} value of -37.0 for HgS(s). Consistent with the results of Benoit et al. (1999), however, in no situation did HgS(s) formation control the aqueous solubility of inorganic Hg.

Inorganic Hg methylation was modeled based on the assumption that sulfate-reducing bacteria (SRB) were the primary agents of Hg methylation (Benoit et al., 2003). Although dissimilatory Fe(III)-reducing bacteria have recently been shown to be capable of methylating Hg (Fleming et al., 2006; Kerin et al., 2006), none of the Everglades sediments considered here showed evidence of significant rates of Fe(III) reduction, and hence this potential pathway for Hg methylation was ignored. Rates of He methylation by SRB were calculated as the product of methylating SRB cell density (in units of cells per mL bulk sediment) and the relationship between cell-specific Hg methylation rate and total neutral aqueous Hg-S complex concentration for *Desulfobulbus propionicus* (1pr3) shown in Fig. 2A of Benoit et al. (2003)

(reproduced in appropriate units in Fig. 5.3 below):

$$R_{HgMeth} = \lambda \times [Cells] \times 2.34 \times 10^{-7} \times [Hg(SH)_2(aq) + HgS(aq)] \times f(DS)$$

where 2.34×10^{-7} is the slope of the line in Fig. 5.3. This formulation explicitly links the abundance of neutral Hg-S species to rates of Hg methylation, which remains the prevailing hypothesis regarding the relationship between aqueous Hg speciation and methylation in sediments (Benoit et al., 2003).

The density of SRB cells was estimated based on simulated rates of SO_4^{2-} reduction and published information on cell-specific metabolic rates for these organisms (Widdel and Bak, 1991). The parameter λ is an adjustable scalar that takes on a value of 0 to 1. This parameter can be altered to depict the propensity of in situ SRB populations to methylate neutral Hg-S complexes relative to pure cultures of *Desulfobulbus propionicus* (1pr3). λ values of 0.1 to 0.3 were used in the simulations described below.

Finally, the term f(DS) was additional included to account in a general way for the inhibitory influence of DS on Hg methylation that were not otherwise captured in this model. Without this term, modeled Hg methylation rates were maximal at mM concentrations, while field observations from the Everglades and other ecosystems show maximal MeHg concentrations at low μM DS concentrations. This empircal factor is justified because the Hg speciation model used in the exercise (the Benoit et al. 1999 model) does not include recently identified complexes that form between neutral dissolved HgS complexes and organic matter under anoxic conditions (Miller et al. 2007). The formation of these complexes may help to explain why sulfide inhibits Hg methylation at relatively low DS concentrations. However, the mechanism of this interaction, including its stoichiometry, is not fully understood, and formation/binding constants for the complex have not been developed. Because the physiochemical mechanism whereby DS inhibits Hg methylation is not known, f(DS) was defined the following empirical manner:

$$f(DS) = 1.0, [DS] \leq [DS]_{critical}$$

$$f(DS) = 1.0 \times \exp(-\alpha[DS]), [DS] > [DS]_{critical}$$

where $[DS]_{critical}$ is the DS concentration above which sulfide inhibition of Hg methylation is assumed to take place. $[DS]_{critical}$ was set equal to values of 10 μM based on our studies of sediments in the Everglades and other ecosystems. A fixed value of 0.2 was assumed for α.

MeHg demethylation was modeled as a simple first-order rate process acting on the dissolved MeHg pool. A fixed value of 0.2 was assumed for $k_{MeHgDemeth}$, based on the results given for Everglades sediments in Marvin-DiPasquale et al. (2000).

Application of Diagenetic Model to Everglades Sediments

The general procedure for calibrating the model for a given site is described below. We then

explain in some detail the application of the model to the different Everglades sites, including site 3A15 for which non-steady-state simulations were conducted in order to provide inputs for the E-MCM simulations discussed in the final section of this report.

Calibration to Sediment Sulfur Chemistry. Since SRB were assumed to be the primary agents of Hg methylation, and since the abundance of dissolved sulfide (DS) has a major impact on dissolved inorganic Hg concentration and methylation rate (vis-à-vis the formation of neutral Hg-S complexes), it was important to be able to reproduce the observed porewater SO_4^{2-} and HS^- profiles as well as possible before optimizing the simulation of Hg transformation and speciation. Model testing showed that in all cases, based on the observed CO_2+CH_4 production rates and/or $^{35}SO_4^{2-}$-based sulfate reduction rates, simple diffusive transport could not account for the required input of SO_4^{2-} to the sediment; in other words, additional transport processes must have been active in order to provide the required supply of SO_4^{2-}. The influence of sediment macrofauna (e.g. insects) and methane gas bubble ebullition on solute transport in wetland soils and aquatic sediments is a well-documented phenomenon (Matisoff, 1995). Increasing the effective rate of diffusive flux to account for enhanced transport associated with such processes is a standard approach in diagenetic modeling (Boudreau, 1997). This is achieved through the use of "irrigation coefficient" (D_{irr}), which is added to the sediment diffusion coefficient for each dissolved species. The D_{irr} values required to reproduce observed SO_4^{2-} and HS^- profiles in Everglades sediments (see below) were ca. 10 to 100-fold higher than average solute molecular diffusion coefficients.

Another factor that can have an important impact on sediment aqueous/solid-phase sulfur speciation is the formation of solid-phase iron-sulfide (referred to collectively here as $FeS_x(s)$) compounds such as FeS(s) (iron monosulfide) and $FeS_2(s)$. Wet chemical analyses have clearly documented the presence of such compounds in Everglades sediments. Formation of $FeS_x(s)$ phases via reactions such as

$$Fe^{2+} + HS^- = FeS(s) + H^+$$

$$FeS + HS^- + 0.5O_2 + H^+ = FeS_2(s) + H_2O$$

may limit the concentration of DS and thereby have an important impact on Hg speciation and biotransformation. For the simulations reported here, the abundance of sediment Fe compounds that could react with DS to form $FeS_x(s)$ was set equal to the average observed total concentration of Fe-S compounds (expressed in Fe equivalents). These values were consistently higher than concentrations of dilute acid-extractable Fe, which suggests that virtually all of the reactive Fe pool have been converted to stable $FeS_x(s)$ compounds such as $FeS_2(s)$. The simulations reported here were run for a period of time sufficient to convert all of the initial pool of reactive Fe to $FeS_x(s)$ compounds, such that the concentration of DS in sediment porewater was determined mainly by the balance between production, reoxidation, and transport. Once a reasonable fit to the porewater SO_4^{2-} and DS profiles was achieved, the parameters associated with Hg transformation were adjusted as described next.

Calibration to Sediment Hg Chemistry. The partitioning of inorganic Hg between aqueous and solid-phase was controlled according to the Benoit et al. (1999) solid-phase model (see above). The stability constants for formation of the Hg-S surface complexes needed to be adjusted only minimally from the best-fit values for Everglades sediments reported in Benoit et al. (1999) to obtain reasonable agreement with the observed values. The parameter λ was then adjusted to achieve agreement between predicted and observed values for the fraction of total sediment Hg present as methyl-Hg. Finally, the partition coefficient for methyl-Hg sorption was

adjusted to achieve dissolved methyl-Hg concentrations comparable to observed values.

Simulation Results

Sites U3 and F1 in WCA 2. The model was first applied to sites U3 and F1 in WCA 2A. Northern WCA 2A surface waters exhibit some of the highest sulfate and phosphate concentrations in the EPA. Key parameter values used to obtain reasonable model predictions of the observed sediment S and Hg biogeochemistry are listed in Table 5.4, and the results of the simulations are shown in Fig. 5.4. The results of these simulations were quite promising, in that it was possible to obtain better than order-of-magnitude accuracy on the very low concentrations of dissolved inorganic Hg, sorbed/dissolved methyl-Hg.

Cells 1-3 in STA 3/4. The model was next applied to data from three sites (Cells 1A,B, 2A,B, and 3A,B) in STA 3/4 located northwest of WCA 2. Key parameter values used to obtain reasonable model predictions of the observed sediment S and Hg biogeochemistry are listed in Table 5.4, and the results of the simulations are shown in Fig. 5.5. Although (for reasons whose explanation is beyond the scope of this report) it was not possible to model aqueous and solid-phase S distributions with a high degree of accuracy in these sites, the model nevertheless accurately reproduced the observed aqueous and solid-phase Hg data.

Site 3A-15 in WCA 3. The final application of the model was to site 3A15 in WCA 3A, which has been studied by our research team for over a decade through the ACME and other programs. Key parameter values used to obtain reasonable model predictions of the observed sediment S and Hg biogeochemistry are listed in Table 5.4, and the results of the simulations are shown in Fig. 5.6. The model predictions matched the observed data from 1996 and 1998 quite well. These results lend confidence to the trends in sediment methyl-Hg content predicted below based on the changing abundance of sulfate in 3A15 surface waters.

Predicted vs. Observed Sediment Methyl-Hg. Fig. 5.7 shows the predicted vs. observed depth-averaged ratio of methy-Hg to total Hg in the four different Everglades sediments considered in the modeling exercise. The close correspondence between the predicted and observed data was expected based on the ability of the calibrated models to reproduce the observed depth distributions of aqueous and solid-phase inorganic and methyl-Hg (Figs. 5.4-6).

Predicted Response of 3A15 Sediments to Changing Surface Water Sulfate. The predicted depth distributions of sulfur and Hg species shown in Fig. 5.6 were used (along with all the other predicted distributions) as the starting conditions for a 10-year, non-steady-state simulation of the response of 3A15 sediments to changes in surface water sulfate abundance documented for this site between 1995 and 2005. Fig. 5.8A shows the changing sulfate concentrations over time that served as input to the model, and Fig. 5.8B shows the predicted response in terms of the depth-averaged fraction of total sediment Hg accounted for by methyl-Hg. Although the predictions do not precisely match the highly variable observed data, the basic trend of decreasing methyl-Hg with decreasing sulfate abundance is similar. These results suggest that changes in the abundance or activity of Hg-methylating SRB could be responsible for the decline in methyl-Hg abundance in 3A15 sediments observed over the past 10 years. The inset in Fig. 5.8A shows the predicted depth-averaged sulfate concentration, DS concentration, and sulfate reduction rate (SRR) over time which served as inputs to the E-MCM simulations.

Table 5.1. Primary dependent variables included in the diagenetic model.

Variable	Fortran Name	Units
O_2	O2	μmol mL_{aq}^{-1}
Fe(III)(s)	Fe3	μmol g dry sed^{-1}
Fe(II)(aq)	Fe2aq	μmol mL_{aq}^{-1}
Fe(II)(ads)	Fe2ads	μmol g dry sed^{-1}
CH_4	CH4	μmol mL_{aq}^{-1}
ΣDIC[a]	DIC	μmol mL_{aq}^{-1}
SO_4^{2-}	SO4	μmol mL_{aq}^{-1}
ΣDS[b]	DS	μmol mL_{aq}^{-1}
S^0(s)	S0	μmol g dry sed^{-1}
FeS(s)	FeS	μmol g dry sed^{-1}
HgI(ads)[c]	HgIads	μmol g dry sed^{-1}
HgI(aq)	HgIaq	μmol mL_{aq}^{-1}
HgS(s)	HgS	μmol g dry sed^{-1}
MeHg(ads)[d]	MeHgads	μmol g dry sed^{-1}
MeHg(aq)	MeHgaq	μmol mL_{aq}^{-1}

[a] ΣDIC = Total dissolved inorganic carbon
[b] ΣDS = Total dissolved sulfide
[c] HgI= Inorganic Hg; (ads) = adsorbed; (aq) = aqueous
[d] MeHg = Methyl-Hg

Table 5.2. Computational scheme for use of the "modified Monod" approach to simulate the temporal-spatial sequencing of major TEAPs in Everglades sediments.*

If $[O_2] > [O_2]_{lim}$ Then

$R_{O2} = R_{CH2O}$

$R_{Fe(III)} = R_{SO4} = R_{CH4} = 0$

Else

$R_{O2} = R_{CH2O} \times [O_2]/[O_2]_{lim}$

If $[Fe(III)] > [Fe(III)]_{lim}$ Then

$R_{Fe(III)} = (R_{CH2O} - R_{O2})$

$R_{SO4} = R_{CH4} = 0$

Else

$R_{Fe(III)} = (R_{CH2O} - R_{O2}) \times [Fe(III)]/[Fe(III)]_{lim}$

If $[SO_4^{2-}] > [SO_4^{2-}]_{lim}$ Then

$R_{SO4} = (R_{CH2O} - R_{O2} - R_{Fe(III)})$

$R_{CH4} = 0$

Else

$R_{SO4} = (R_{CH2O} - R_{O2} - R_{Fe(III)}) \times [SO_4^{2-}]/[SO_4^{2-}]_{lim}$

$R_{CH4} = (R_{CH2O} - R_{O2} - R_{Fe(III)} - R_{SO4})$

End If

End If

End If

---

* Adapted from Van Cappellen and Wang (1995; 1996). RCH2O represents the total collective rate of all TEAPs in units of μmol C per mL bulk sediment per day. RO2, RFe(III), RSO4, and RCH4 refer to rates of OC oxidation coupled to O2 reduction (aerobic respiration), Fe(III) oxide reduction, SO42- reduction, and methanogenesis, respectively. The subscript "lim" refers to the limiting concentration for a given EA (in units of μmol per mL bulk sediment).

Table 5.3. Tableau of components and species in the equilibrium speciation system included in the diagenetic model.

			1	2	3	4	5	6	7	
		Components:	HCO3(-)	Fe (2+)	HS(-)	Hg(2+)	ROH	XOH	H (+)	log K
Species:	1	H2CO3 (aq)	1	0	0	0	0	0	1	6.35
	2	HCO3 (-)	1	0	0	0	0	0	0	0
	3	CO3 (2-)	1	0	0	0	0	0	-1	-10.33
	4	Fe (2+)	0	1	0	0	0	0	0	0
	5	FeOH(+)	0	1	0	0	0	0	-1	-9.5
	6	FeHCO3 (+)	1	1	0	0	0	0	0	2
	7	FeCO3 (aq)	1	1	0	0	0	0	-1	-4.83
	8	Fe(CO3)2 (2-)	2	1	0	0	0	0	-2	-3.23
	9	H2S(aq)	0	0	1	0	0	0	1	6.99
	10	HS(-)	0	0	1	0	0	0	0	0
	11	S(2-)	0	0	1	0	0	0	-1	-12.92
	12	Hg(2+)	0	0	0	1	0	1	0	0
	13	Hg(SH)2(aq)	0	0	2	1	0	0	0	37.5
	14	HgS2H(-)	0	0	2	1	0	0	-1	32
	15	HgS2(2-)	0	0	2	1	0	0	-2	23.5
	16	HgSH(+)	0	0	1	1	0	0	0	30.5
	17	HgS(aq)	0	0	1	1	0	0	-1	26.5
	18	ROH[a]	0	0	0	0	1	0	0	0
	19	RSHg(+)	0	0	1	1	1	0	0	38
	20	(RS)2Hg	0	0	2	1	2	0	0	42
	21	XOH[b]	0	0	0	0	0	1	0	0
	22	XO-Hg	0	0	0	1	0	1	0	30
	23	OH (-)	0	0	0	0	0	0	-1	-14
	24	H (+)	0	0	0	0	0	0	1	0

[a] ROH = Solid-phase site capable of forming complex with Hg^{2+} and HS^-

[b] XOH = Solid-phase site capable of forming complex with Hg^{2+} alone

Table 5.4. List of key parameter values used in Everglades sediment diagenetic models.

Site	Parameter	Description	Value	Units	Source
U3	SO4sw	Surface water sulfate concentration	0.084	μmol mLaq-1	Observed
U3	RCH2O0	Total rate of POC decay at sediment surface	0.434	μmol mLbulk-1d-1	Fig. 5.2
U3	αPOC	Coefficient for decline in POC decay rate with depth	0.171	cm-1	Fig. 5.2
U3	O2sw	Surface water dissolved O2 concentration	0.01	μmol mLaq-1	Adjustable
U3	Dirr	Porewater irrigation coefficient	5 × 10-4	cm2 s-1	Adjustable
U3	λ	Scalar for calculation of Hg-S methylation (see text)	0.1	unitless	Adjustable
U3	Kd,MeHg	Aqueous/solid-phase partition coefficient for methyl-Hg	103	unitless	Adjustable
F1	SO4sw	Surface water sulfate concentration	0.140	μmol mLaq-1	Observed
F1	RCH2O0	Total rate of POC decay at sediment surface	0.434	μmol mLbulk-1d-1	Fig. 5.2
F1	αPOC	Coefficient for decline in POC decay rate with depth	0.171	cm-1	Fig. 5.2
F1	O2sw	Surface water dissolved O2 concentration	0.01	μmol mLaq-1	Adjustable
F1	Dirr	Porewater irrigation coefficient	2 × 10-4	cm2 s-1	Adjustable
F1	λ	Scalar for calculation of Hg-S methylation (see text)	0.1	unitless	Adjustable
F1	Kd,MeHg	Aqueous/solid-phase partition coefficient for methyl-Hg	103	unitless	Adjustable
STA 3/4 a	SO4sw	Surface water sulfate concentration	0.06	μmol mLaq-1	Observed
STA 3/4	RCH2O0	Total rate of POC decay at sediment surface	0.434	μmol mLbulk-1d-1	Fig. 5.2
STA 3/4	αPOC	Coefficient for decline in POC decay rate with depth	0.171	cm-1	Fig. 5.2
STA 3/4	O2sw	Surface water dissolved O2 concentration	0.05	μmol mLaq-1	Adjustable
STA 3/4	Dirr	Porewater irrigation coefficient	3 × 10-4	cm2 s-1	Adjustable
STA 3/4	λ	Scalar for calculation of Hg-S methylation (see text)	0.3	unitless	Adjustable
STA 3/4	Kd,MeHg	Aqueous/solid-phase partition coefficient for methyl-Hg	103	unitless	Adjustable
3A15b	SO4sw	Surface water sulfate concentration	0.04	μmol mLaq-1	Observed
3A15	RCH2O0	Total rate of POC decay at sediment surface	0.434	μmol mLbulk-1d-1	Fig. 5.2
3A15	αPOC	Coefficient for decline in POC decay rate with depth	0.171	cm-1	Fig. 5.2
3A15	O2sw	Surface water dissolved O2 concentration	0.001	μmol mLaq-1	Adjustable
3A15	Dirr	Porewater irrigation coefficient	5 × 10-3	cm2 s-1	Adjustable
3A15	λ	Scalar for calculation of Hg-S methylation (see text)	0.1	unitless	Adjustable
3A15	Kd,MeHg	Aqueous/solid-phase partition coefficient for methyl-Hg	103	unitless	Adjustable

a Data from cells 1-3 in STA 3/4 were considered collectively during modeling of the data from this site.
b Data from four different sampling campaigns at 3A15 (June 1996, December 1996, January 1998, and December 1998) were considered collectively during modeling of the data from this site.

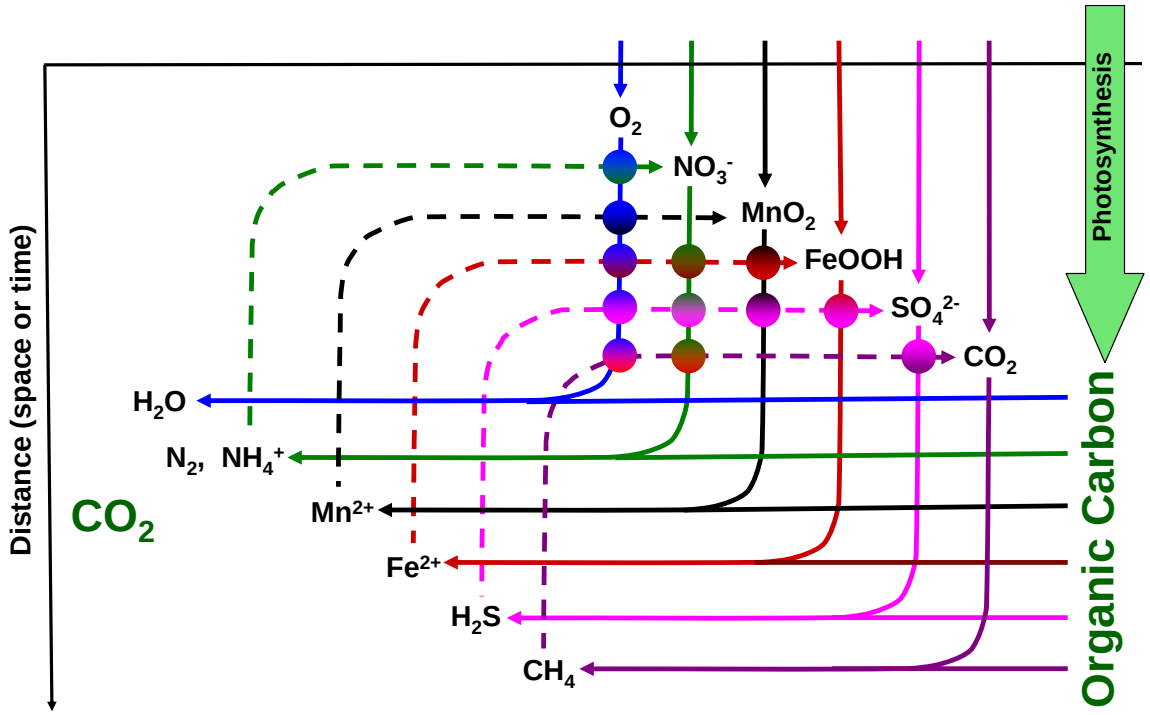

Figure 5.1. Interaction of C, O, N, Mn, Fe, and S redox cycles in sediments. Primary redox reactions are driven by oxidation of organic carbon. Circles at intersections indicate secondary redox reactions between electron acceptors and reduced end-products of anaerobic respiration. Adapted from Thamdrup & Canfield (2000).

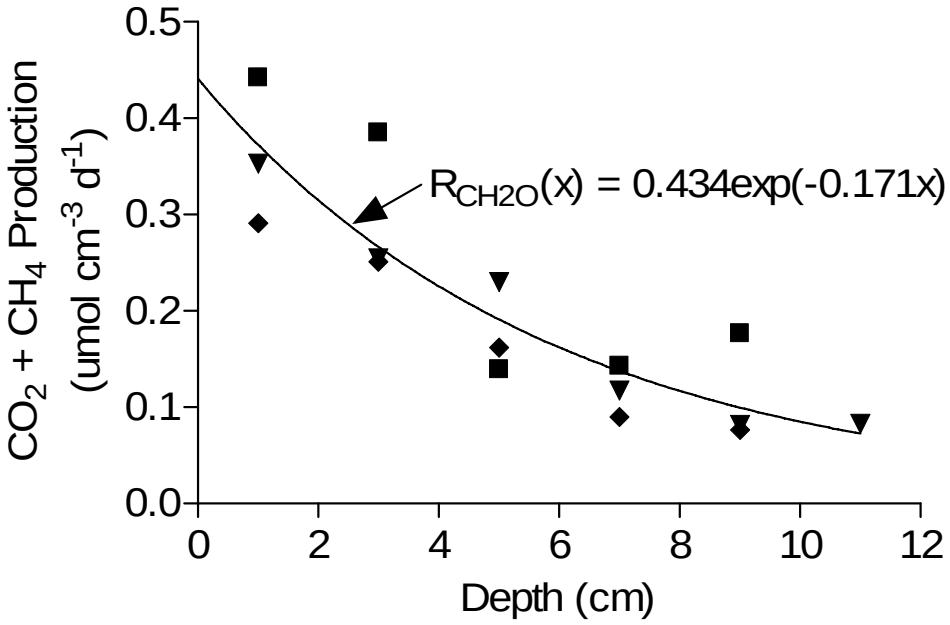

Figure 5.2. Depth distribution of total CO_2 + CH_4 production rate in sediments from STA 3/4. Squares, trianges, and diamonds show results for cells 1, 2, and 3, respectively. The solid lines shows a nonlinear least-squares regression fit of the pooled data.

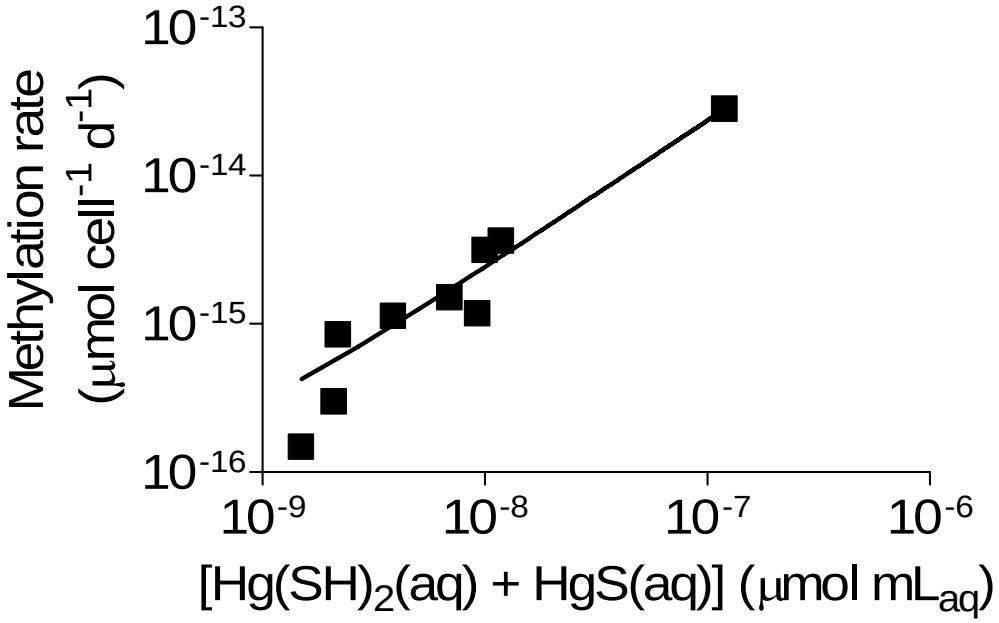

Figure 5.3. Rates of HgI methylation by *Desulfobulbus propionicus* (1pr3) as a function of calculated neutral aqueous Hg-S complex concentration. Modified from Fig. 2A in Benoit et al. (2003).

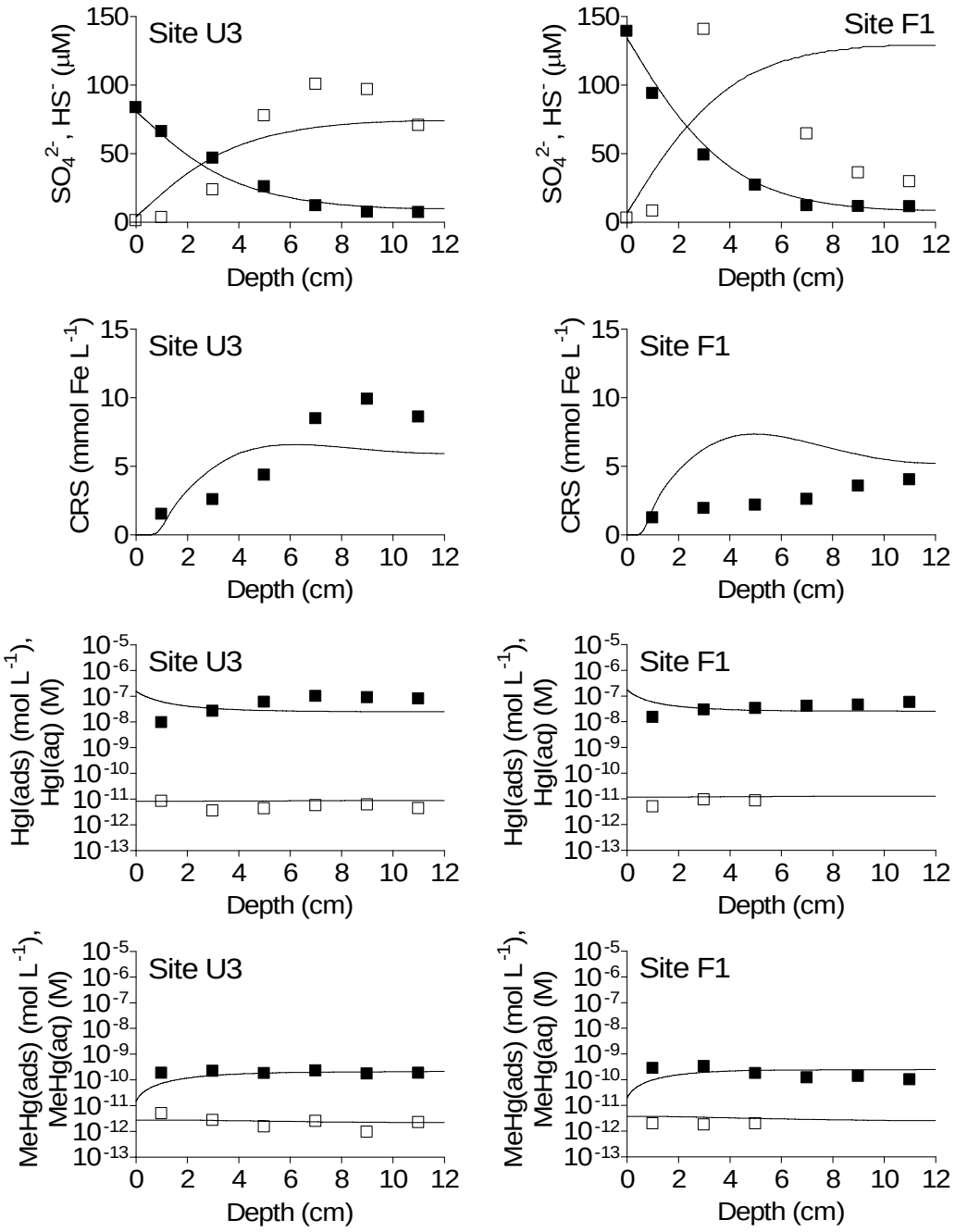

Figure 5.4. Observed (symbols) and simulated (lines) depth distributions of porewater sulfate/sulfide, solid-phase reduced sulfur (in Fe equivalents), aqueous/solid-phase inorganic Hg, and aqueous/solid-phase methyl-Hg in U3 and F1 sediments. Solid and open symbols show solid-phase and aqueous concentrations, respectively. Sediment data were collected in June 2005.

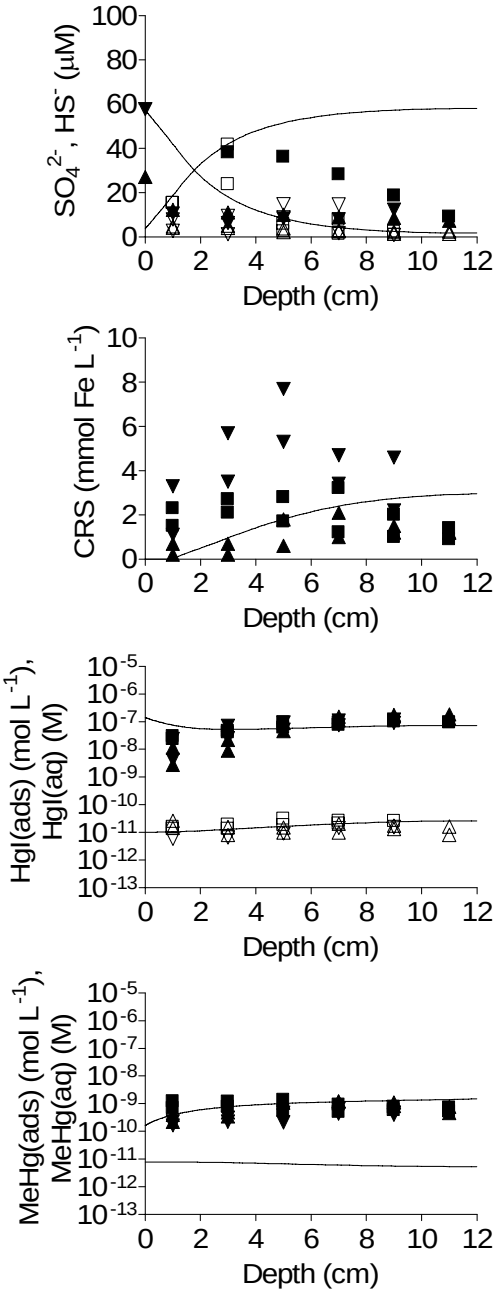

Figure 5.5. Observed (symbols) and simulated (lines) depth distributions of porewater sulfate/sulfide, solid-phase reduced sulfur (in Fe equivalents), aqueous/solid-phase inorganic Hg, and aqueous/solid-phase methyl-Hg in STA 3/4 sediments. Solid and open symbols show solid-phase and aqueous concentrations, respectively. Squares, triangles, and upside-down trianges show data from cells 1, 2, and 3, respectively. Sediment data were collected in May 2004; no measurements of aqueous MeHg were obtained during this campaign.

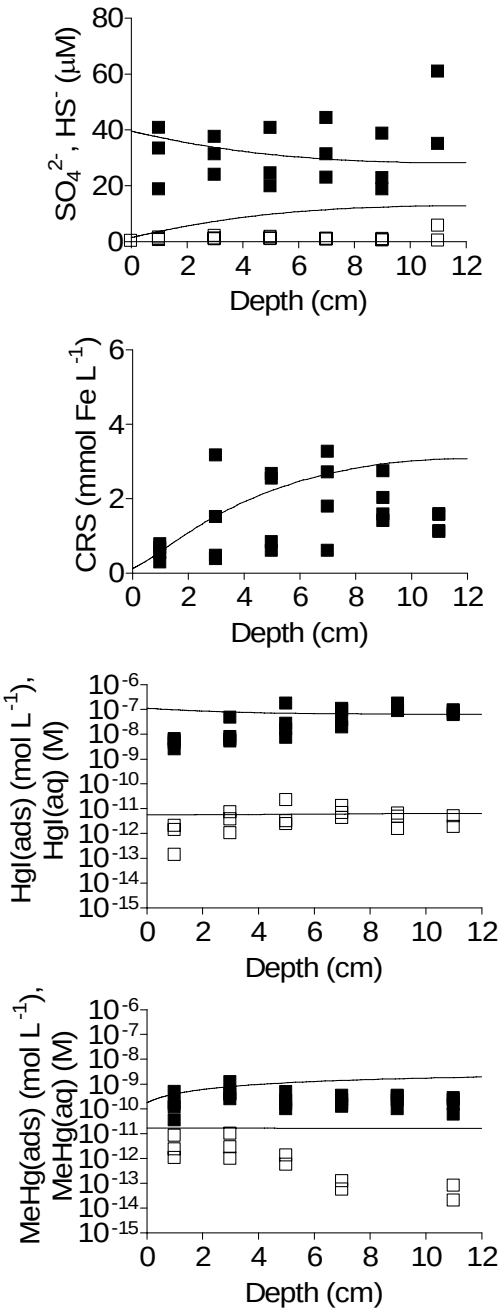

Figure 5.6. Observed (symbols) and simulated (lines) depth distributions of porewater sulfate/sulfide, solid-phase reduced sulfur (in Fe equivalents), aqueous/solid-phase inorganic Hg, and aqueous/solid-phase methyl-Hg in 3A15 sediments. Solid and open symbols show solid-phase and aqueous concentrations, respectively. Pooled data from sampling campaigns in June 1996, December 1996, January 1998, and December 1998 are shown.

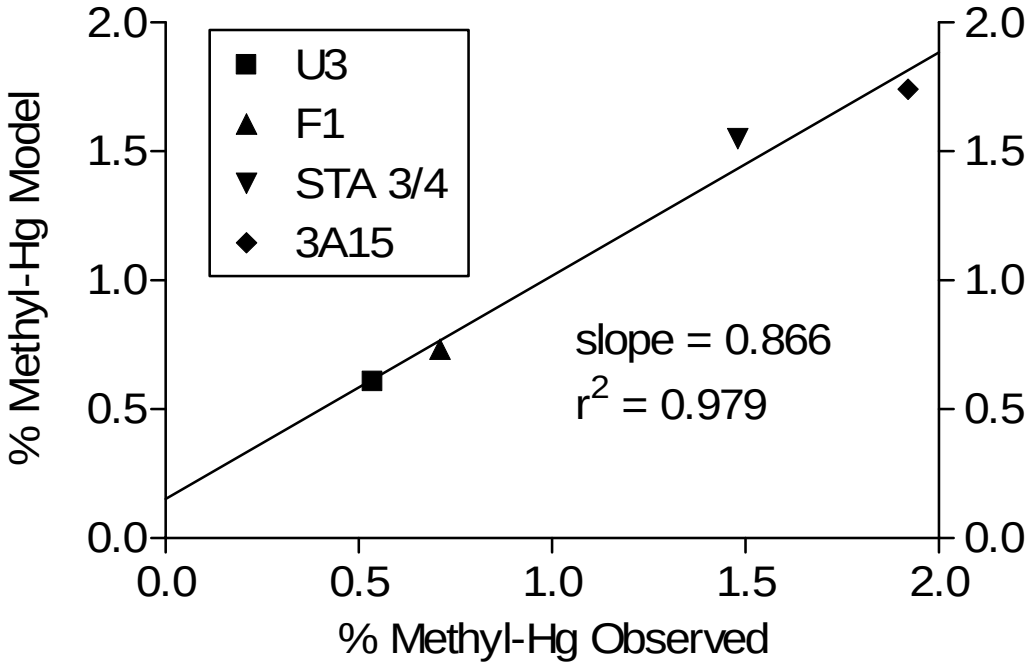

Figure 5.7. Simulated vs. observed depth-averaged ratio of methy-Hg to total Hg (expressed in term of percentage) in the four different Everglades sediments considered in the modeling exercise.

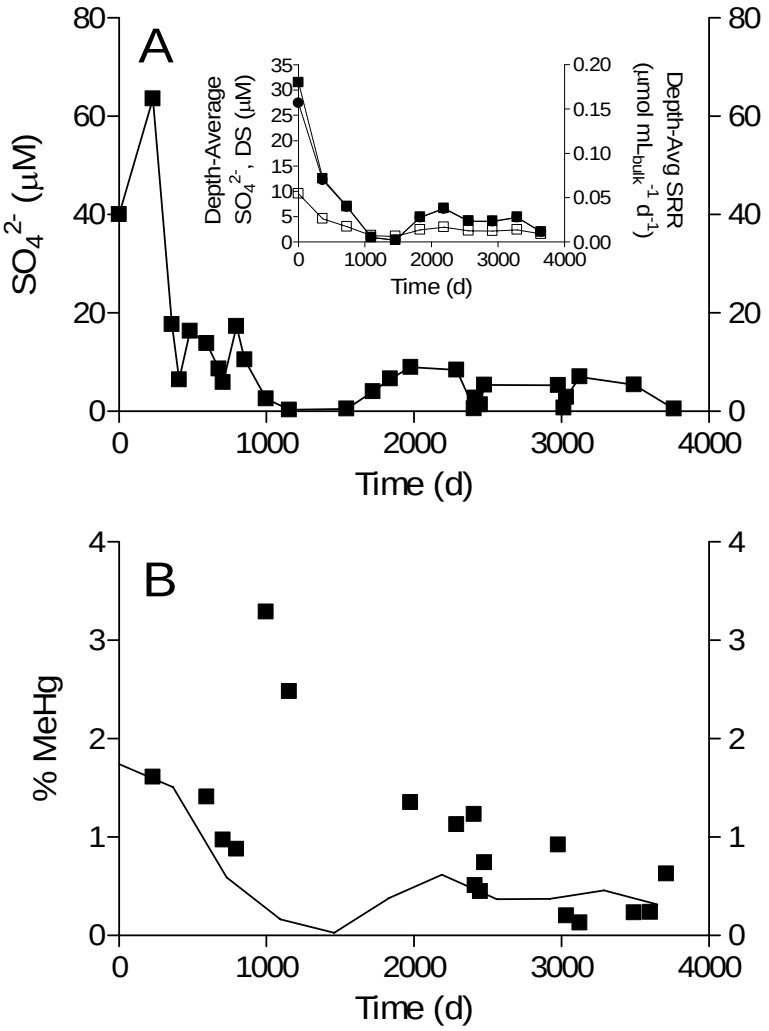

Figure 5.8. Changes in surface water sulfate concentration at site 3A15 for a ca. 10-year time period between 1995 and 2005 (A), and the non-steady-state model-predicted response of sediment methyl-Hg abundance to those changes (B). The steady-state sediment sulfur and Hg distributions shown in Fig. 6 were used as starting conditions for the non-steady-state simulations. The inset in panel A shows the predicted depth-averaged SO_4^{2-} concentration, DS concentration, and sulfate reduction rate (SRR) over time which served as inputs to the E-MCM simulations.

TASK 6. EXAMINING THE ROLE OF SULFUR ON METHYLATION: E-MCM SIMULATIONS AT WCA 3A-15

Objective

Explore ways to improve the ability of the Everglades Mercury Cycling Model (E-MCM) to predict relationships between sulfate and methylmercury production and bioaccumulation in the Everglades. Specifically, test whether a more mechanistic treatment of sulfur cycling improves the predictive strength of the model, using output from the diagenetic model developed in Task 5.

Introduction

Mechanistic simulation models provide a useful tool to investigate factors controlling key processes in the mercury cycle, including the effects of sulfur cycling on methylation rates. An existing model of mercury cycling and bioaccumulation in Everglades marshes, the Everglades Mercury Cycling Model (E-MCM, Tetra Tech 1999) includes algorithms to represent microbial methylation of mercury, but it is unresolved how to best link methylation to sulfur cycling. E-MCM treats methylation as being governed by two basic factors: (1) the activity of methylating microbes, and (2) the concentration of inorganic Hg(II) that is available to methylating organisms. The activity of methylating microbes is currently roughly represented by using overall mass decomposition rates as a surrogate, with an option to include a sulfate concentration dependency. The sulfate effect in E-MCM, modeled using Michaelis-Menten kinetics, is typically linear at low sulfate levels, but has no effect once sulfate concentrations are sufficiently elevated. The concentration of inorganic Hg(II) available for methylation is predicted in E-MCM using thermodynamic speciation, including complexation of mercury by sulfide species. Currently the model requires users to provide time-series concentrations of total sulfide concentrations, and uses this in the thermodynamic routines.

In this study, existing methylation algorithms in E-MCM were compared to an approach that uses estimates of sulfate reduction rates derived from a diagenetic model of sulfur cycling in task 5. The ability of existing E-MCM algorithms to predict sulfide effects on mercury availability for methylation was also examined.

E-MCM has been previously applied to Water Conservation Area (WCA) 3A-15 as part of a pilot mercury TMDL exercise (Tetra Tech Inc. 2000), and later updated in 2004 as part of an exercise to hindcast the modern history of mercury loadings to the site (Axelrad et al. 2005; C. Pollman, unpublished data). However neither of these model applications used an equation for methylation that directly related the process to sulfate reduction rates. In both exercises, methylation rates depended on the total dissolved Hg concentration in pore water.

Because of the previous calibration of E-MCM to site 3A15, and because surface water sulfate and MeHg concentrations in water, soil and fish have declined at WCA 3A15 over the period for which data are available (1995-2005; 2007 South Florida Environmental Report Chapter 3 and Appendices 3B-2 and 3B-2), this site was used to test approaches to modeling the dependency of methylation on sulfate within E-MCM.

Overview of E-MCM

The Everglades Mercury Cycling Model (E-MCM) (Tetra Tech 2003, Tetra Tech 1999) simulates mercury cycling and bioaccumulation in marsh areas of the Florida Everglades. E-MCM accommodates unique features of Everglades marshes, including shallow waters, a system of canals and managed water levels, a warm subtropical climate, high sun exposure, neutral to alkaline pH, high concentrations of dissolved organic carbon, large biomass of aquatic vegetation including periphyton, sawgrass, cattails and water lilies, and a wide range of nutrient levels and primary productivity.

E-MCM is a mechanistic simulation model that runs on Windows™-based computers. Using a mass balance approach, the model predicts time-dependent concentrations for three forms of mercury: inorganic Hg(II), methylmercury and elemental mercury. Mercury concentrations in the atmosphere are input as boundary conditions to calculate fluxes across the air/water interface (gaseous, wet deposition, dry particle deposition, deposition of reactive gaseous mercury). Model compartments include the water column (dissolved and particular phases), three macrophyte species (cattails, sawgrass, water lilies), four sediment layers and a food web. The simplified food web consists of detritus, periphyton, phytoplankton, zooplankton, benthos, shrimp, mosquitofish (*Gambusia*), bluegill/warmouth sunfish (grouped together), and largemouth bass. Fish mercury concentrations tend to increase with age, and are therefore followed in each year class (up to 20 cohorts) for each species. Bioenergetics equations developed for individual fish at the University of Wisconsin (Hewett and Johnson 1992) were modified to consider temperature dependent growth and coupled to methylmercury fluxes (Harris and Bodaly 1998). These fluxes for individual fish are then adapted to simulate year classes and entire populations (Tetra Tech 1999)

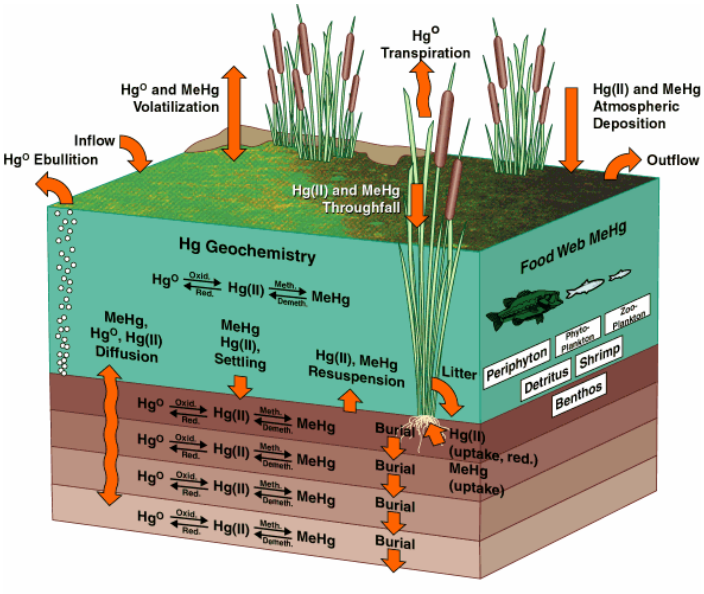

Figure 6.1. Mercury Cycling in E-MCM

Major processes included in E-MCM are shown in Figure 6.1. These processes include surface inflows and outflows, vertical groundwater flow, instantaneous methylmercury partitioning between abiotic solids and dissolved complexes, instantaneous and slower adsorption/desorption kinetics for Hg(II) on abiotic solids, particulate settling, resuspension and burial, macrophyte related fluxes (throughfall, litter, root uptake, transpiration), atmospheric deposition, air/water gaseous exchange, in-situ transformations (methylation, demethylation, MeHg photodegradation, Hg(II) photoreduction), mercury kinetics in plankton, and methylmercury fluxes in fish populations (uptake via food and water, excretion, egestion, mortality, fishing).

E-MCM also has thermodynamic routines to speciate dissolved mercury among various organic and inorganic complexes, including sulfide-mercury complexes. This speciation is used to test hypotheses regarding Hg complexes available for various reactions, including methylation.

E-MCM has been applied to a range of Everglades conditions, including Water Conservation Area 3A-15 as a component of a pilot mercury TMDL exercise (Atkeson *et al.,* 2003), Sites F1 and U3 in Water Conservation Area 2A, the Everglades Nutrient Removal Project (ENR), and Stormwater Treatment Area 2 (STA-2) (Tetra Tech 2003).

Study approach

The overall modeling approach was to examine potential linkages between two aspects of sulfur cycling and methylation: (1) sulfate reduction and (2) sulfide effects on Hg(II) complexation.

Modeling the linkage between sulfate reduction and methylation.

The original calibration of E-MCM at WCA 3A-15 as part of a pilot mercury TMDL (Tetra Tech 2003) was done at a time when there were insufficient data to discern temporal trends in sulfate and MeHg. As a result E-MCM was originally calibrated on the assumption that site conditions and mercury concentrations were stable over time. Subsequent longer records of measurements made it clear that site conditions (e.g. sulfate) changed significantly with time. The steady state assumption was not valid and it was necessary to calibrate E-MCM to dynamic, changing conditions. This was originally done as part of a hindcasting exercise attempting to reconstruct mercury loading patterns at WCA 3A-15 (C. Pollman, unpublished data, Axelrad et al. 2005). During the hindcast simulations, methylation was modeled as a function of porewater sulfate concentrations, but not as a direct function of sulfate reduction rates. In this study, we extended previous calibrations at WCA 3A-15 by comparing results with the following approaches to methylation:

a) Methylation is not affected by sulfate

b) Methylation is related to observed sulfate concentrations, using existing options in the E-MCM framework. Specifically, MeHg concentrations are modeled as a function of

sulfate concentration, overall decomposition rate, available Hg and a tunable methylation rate constant. In this scenario, available Hg is total dissolved Hg.

c) Methylation is related to sulfate reduction rates predicted by the Task 5 diagenetic model. In this case, MeHg concentration is a function of sulfate reduction rate, available Hg and a tunable methylation rate constant. This is a simpler formulation than b) above, but depends on an external model of sulfate reduction rate for input.

Concentrations of MeHg in water and fish were used as the points of comparison. Simulations were carried out for the period 1995 through 2003, based on data availability. A representative 1 km 2 x 1 km2 marsh area was simulated. The site was simulated as a single "cell", i.e. conditions were assumed to be the same horizontally anywhere at the site.

WCA 3A-15 receives mercury loads from inflows as well as direct atmospheric Hg deposition. Inflow HgT and MeHg loads had to be inferred from limited data at site 3A33 from 1996-99 (n=7, USGS data). It was assumed that while the magnitudes of the concentrations in the inflow and in the WCA 3A-15 marsh would differ, the relative concentrations trends would be similar over time. In other words, concentrations would tend to increase or decrease in tandem at both sites with time.

Modeling sulfide-Hg complexation

E-MCM was set up in this study to use the same dissolved Hg-sulfide complexes used by Benoit et al. 1999 and the Task 5 diagenetic model. These are listed in Table 6.1. However, solid phase Hg complexation is coded somewhat differently in E-MCM. Additionally, the model attempted to describe complexation between mercury and dissolved organic matter. To represent the complexation of Hg(II) by dissolved organic carbon, two complexes were considered: $RSHg^{+}$ and $(RS)_2Hg$, both based on unprotonated thiols (RS^{-1}) being the primary binding sites within DOC. These sulfide and DOC complexes competed with other complexes (Table 6.1) and solids for Hg^{++}. Binding of Hg(II) to solids was modeled using an equilibrium partitioning expression that included a term for protonation. Simulations were first carried out for WCA 3A-15 porewater, where sulfide levels are generally <1 uM. Sulfide concentrations were then introduced in the simulations at three environmentally relevant levels: 1 nM, 1 µM, and 1 mM.

Table 6.1. Dissolved ThermodynamicComplexes in E-MCM
Hg(II):
$HgOH$
$Hg(OH)_2$
$HgOHCl$
$HgCl^+$
$Hg(Cl)_2$
$HgRS^+$
$Hg(RS)_2$
HgS (soluble)
HgS (cinnabar)
HgS_2^{--}
$Hg(HS)_2$
$Hg(HS)^+$
$Hg(HS)S^-$
Methylmercury:
CH_3HgOH
CH_3HgCl
CH_3HgRS
CH_3HgS^-
$(CH_3Hg)_2S$

Water Conservation Area 3A-15 Site Description

Water Conservation Area 3A (WCA 3A) in the Everglades is located ~50 km west of Fort Lauderdale and has an area of approximately 1,800 km2 (Figure 6.2). Characteristics of site WCA 3A-15 are summarized in Table 6.2. The site is low in productivity (total phosphorus less than 10 ug L-1), with significant dissolved organic carbon levels (13-19 mg L-1) and circumneutral pH. Sulfate concentrations declined from a maximum of 6 mg L-1 in the mid 1990's to less than 0.1 mg L-1 after 2000 (2007 SFER Appendices 3B-2 and 3B-3). Methylmercury levels in largemouth bass the top trophic level fish species at the site, also declined over that time (2007 SFER Chapter 3). WCA 3A-15 was a site of intense research in the mid to late 1990s after exceptionally high fish mercury concentrations were found in central WCA 3A. Largemouth bass mercury concentrations declined 71 % however from 2.39 ug g-1 (age 3 yr fish) in 1993 to 0.71 ug g-1 by 2005 (Axelrad et al 2007).

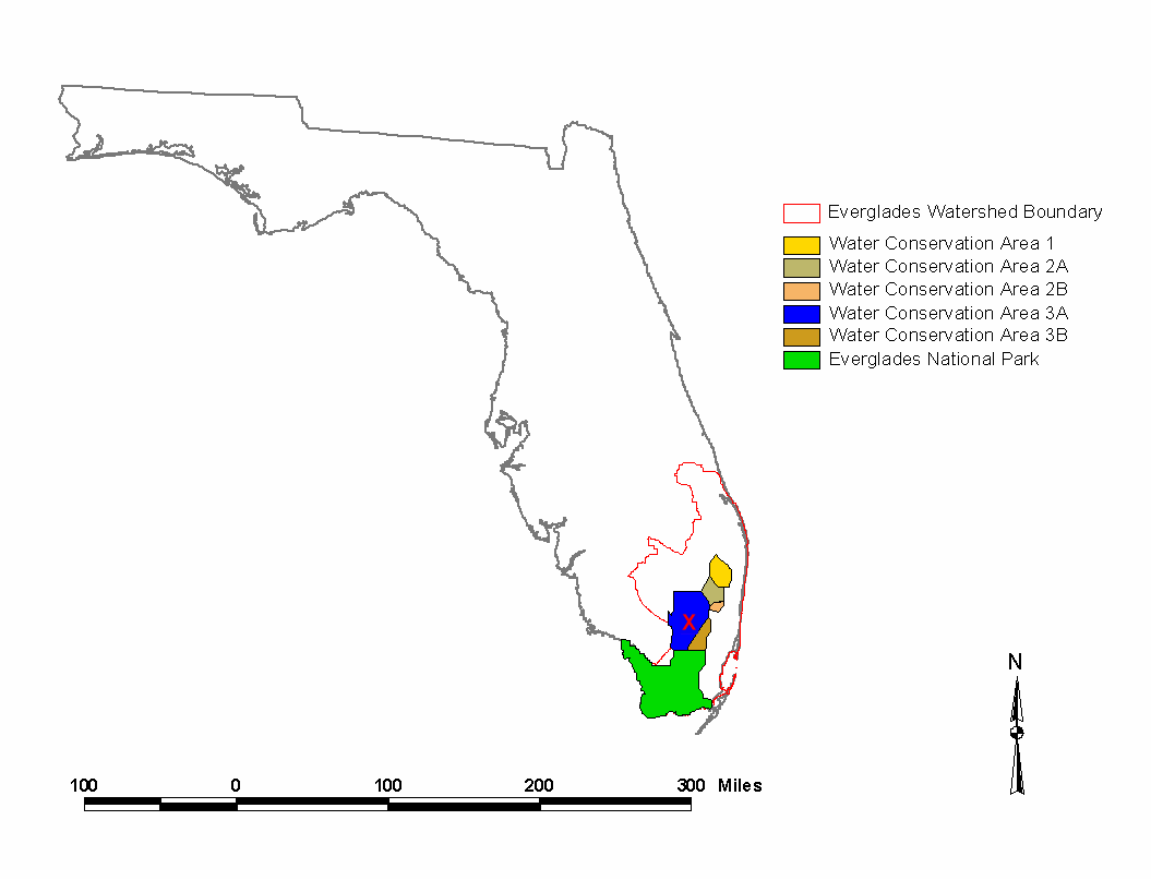

Figure 6.2. Location of Water Conservation Area site 3A-15

Table 6.2. Water Conservation Area 3A-15 Characteristics (1995-2003)	
Parameter	Value
Area modeled	1 km x 1 km
Surface water depth	0.2 to 0.7 m
Air Temperatures (monthly means)	12 to 30 C
Productivity	Low (oligotrophic)
Flow pattern	Surface flow
Stratification	Intermittent
Anoxia	Yes
Dissolved organic carbon	~ 13-19 mg L-1
Surface water pH	~ 6.9-7.3
Surface water chloride	~ 17-36 mg L-1
Surface water sulfate	6.3 to less than 0.1 mg L-1
Sedimentation rate:	< 1 cm yr-1
TSS	~ 2 mg/L
Macrophytes	Primarily sawgrass and water lilies
Fraction of marsh with open water	<50%
Periphyton density	dense
Top predator fish	Largemouth bass

E-MCM Results

Effect of linking methylation to sulfate.

Observed and calibrated concentrations of filtered HgT in WCA 3A-15 surface waters are shown in Figure 6.3. Predicted concentrations differed only slightly between the simulations with methylation depending on sulfate concentration, sulfate reduction rate or having no sulfate dependency. In all cases the calibrated results reasonably matched the overall magnitude and range of the observations.

The calibration of E-MCM to surface water methylmercury concentrations at WCA 3A-15 reflected the observed decline from 1995-2003 and improved when methylation was affected by sulfate (Figure 6.4). While declining surface water methylmercury concentrations were predicted with or without assigning a sulfate dependency for methylation, the extent of decline was greater with a sulfate dependency, and better fit the observations (compare model calibrations to exponential fit to observations in Figure 6.4).

Similar to methylmercury concentrations in water, the extent of decline in mercury concentrations observed for age 1+ (between age 1 and 2 years) largemouth bass was better simulated when methylation was linked to sulfate concentration or reduction rate (Figure 6.5). In the case of young of the year largemouth bass, it was not clear that a sulfate effect on methylation improved the model calibration (Figure 6.6). It is important to note that the predicted fish mercury concentrations in these figures are for age classes, not individual fish. Each year there is a new group of fish that represents a given age class (e.g. age 1+).

For surface water and fish (Figures 6.4, 6.5 and 6.6), modeled MeHg concentrations were similar whether methylation was linked to surface water sulfate concentrations or sulfate reduction rates.

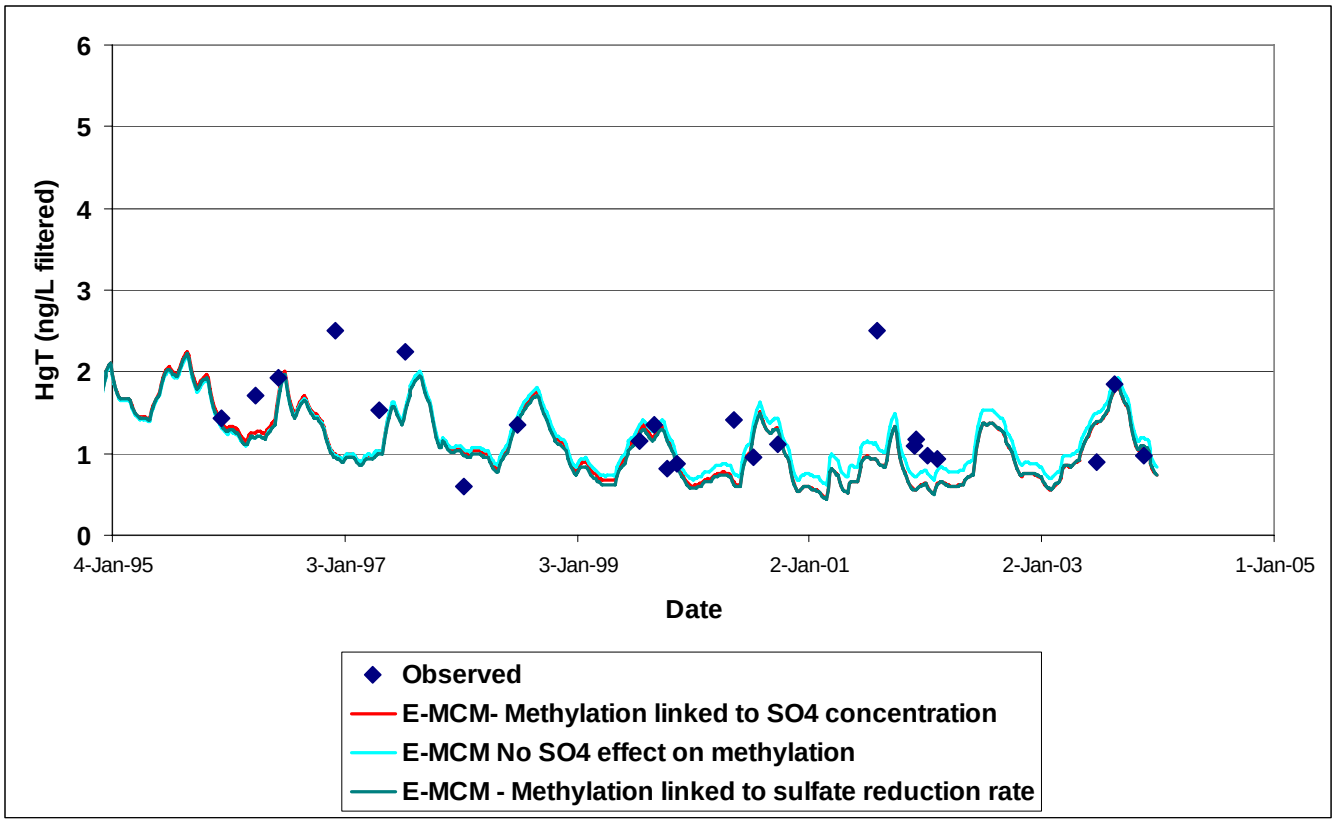

Figure 6.3. Calibrated and observed concentrations of filtered HgT in WCA 3A-15 surface waters 1995-2003. Data from D. Krabbenhoft, USGS.

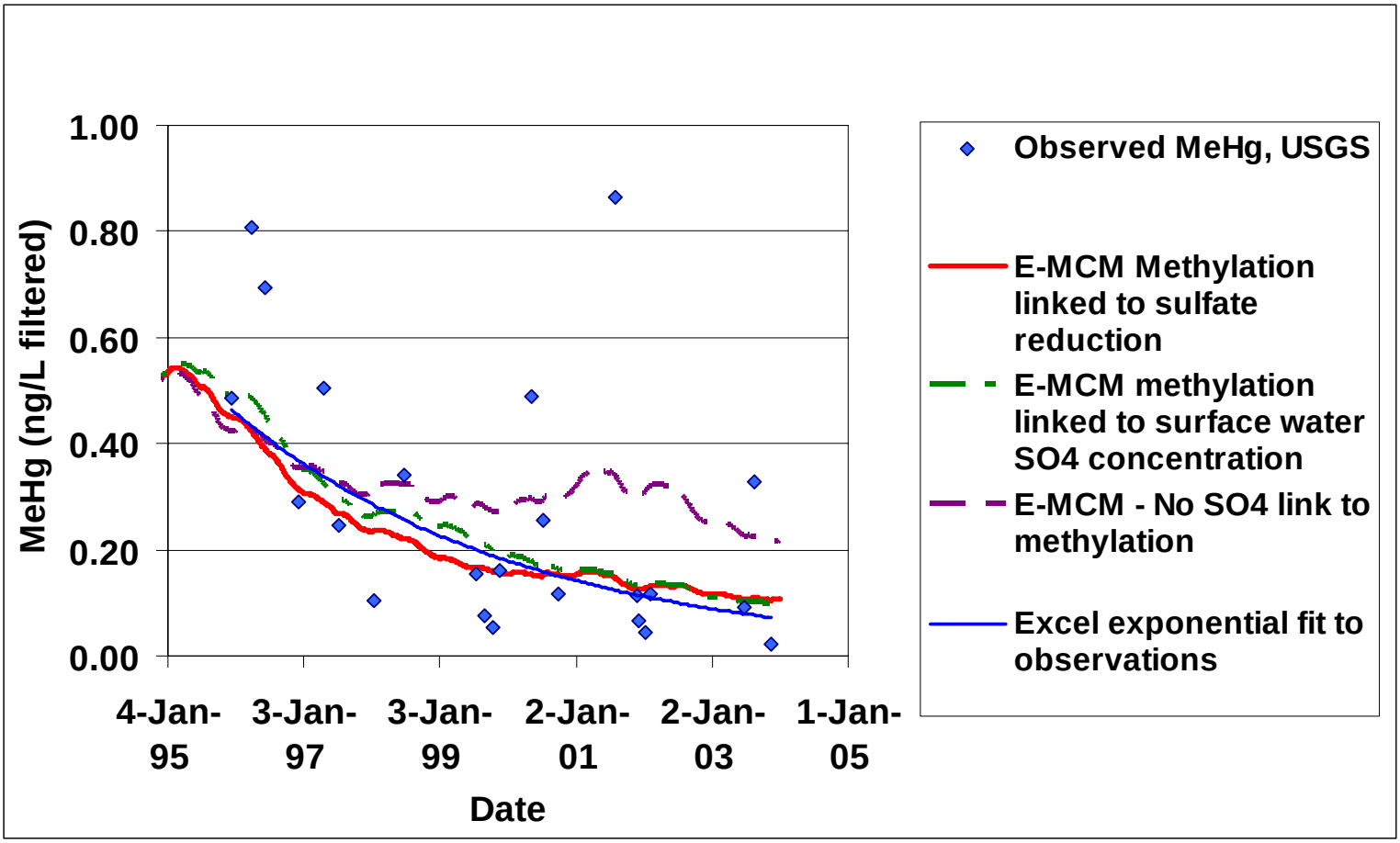

Figure 6.4. Observed and E-MCM calibrated concentrations of methylmercury in WCA 3A-15 surface waters for 1995 -2003. Observations: David Krabbenhoft, USGS.

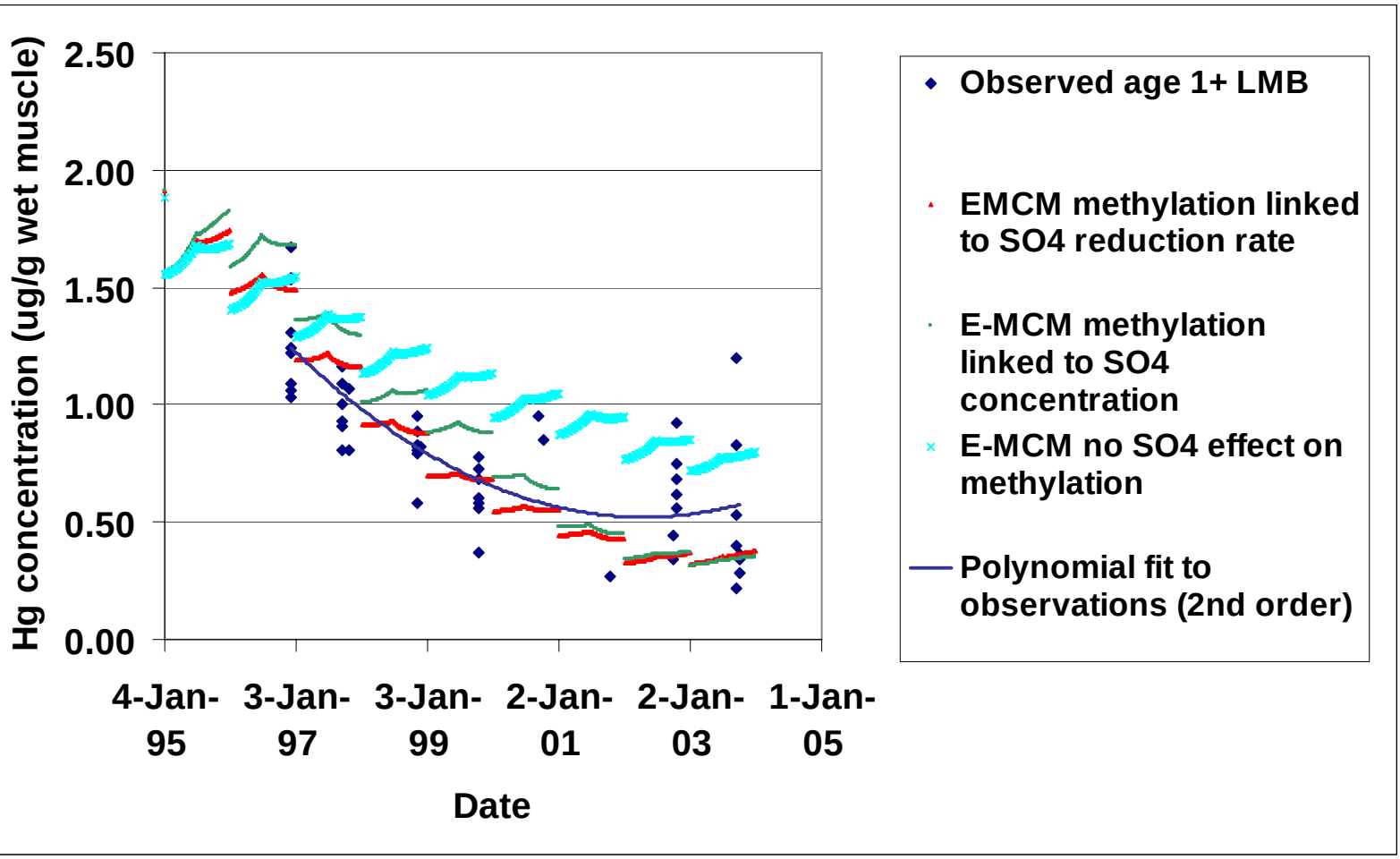

Figure 6.5. Observed and E-MCM calibrated mercury concentrations in age 1+ largemouth bass at WCA 3A-15 1995 -2003. Observations: T. Lange, Florida Fish and Wildlife Conservation Commission

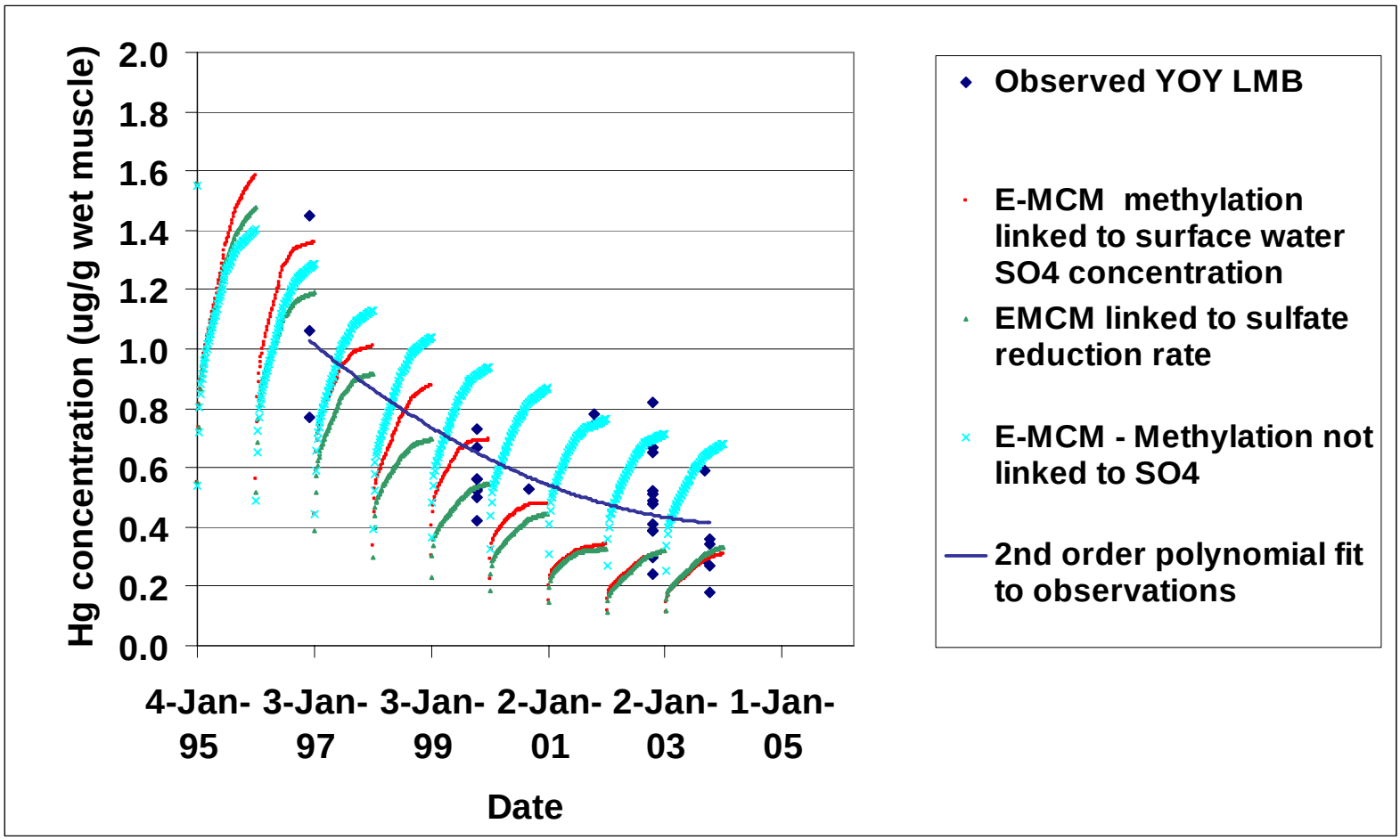

Figure 6.6. Observed and E-MCM calibrated mercury concentrations in young of the year largemouth bass at WCA 3A-15 1995 -2003. Observations: T. Lange, Florida Fish and Wildlife Conservation Commission

Effects of sulfide on methylation – E-MCM

The complexation of Hg with sulfide is important in understanding the production of MeHg in the environment because it has been demonstrated in both laboratory and field studies that sulfide concentrations affect Hg methylation rates through its impact on the bioavailiability of Hg for uptake by Hg methylating microorganisms (Benoit et al. 1999). Importantly, recent research on Hg complexation shows that previously unidentified complexes between Hg, sulfide and dissolved organic matter form, and are dominant, under anaerobic conditions (Hsu-Kim and Sedlak, 2005; Miller 2006; Miller et al. 2007; Miller et al in prep).

In this exercise, the complexation between Hg and DOM is represented by the interaction of Hg with thiols in DOM, which has been the prevailing paradigm for Hg-DOM interactions (e.g. Haitzer et al. 2002). Simulations were carried out with sulfide concentrations ranging from 0 to the mM range. To represent the complexation of Hg(II) by dissolved organic carbon, two complexes were considered: $RSHg^{+}$ and $(RS)_2Hg$, Initial simulations of the effects of sulfides on Hg(II) complexation caused unrealistic shifts away from DOC. These simulations included only 1:1 complexes between Hg and thiols in organic matter ($RSHg^{+}$). Under these circumstances, the sulfide-Hg complexes were unrealistically dominant, with very little Hg bound to DOC or solids. E-MCM was then recalibrated by introducing $(RS)_2Hg$ (Dyrssen and Wedborg, 1991). A complexation constant of approximately 47 (i.e. $(RS)_2Hg = (RS-)^2 * Hg++ * (10)^{47}$) was needed to create conditions where charged Hg-sulfides would not dominate at low sulfide levels (e.g. nM to µM, Figure 6.7), but would eventually dominate Hg(II) speciation if present in sufficient quantity (e.g. mM, Figure 6.8). Dyrssen and Wedborg (1991) estimated a complexation constant of 41.5 for this complex. In this simulation, Hg complexation with dissolved organic matter is modeled as Hg(2+) complexation with thiols in DOM. The content of thiols in DOC was estimated at 1% by weight, or about 10^{-6}M, However, the S content of DOC varies significantly with its source and age (Haitzer et al. 2002) and as does the fraction of total S as free thiols.

Neutral dissolved HgS complexes are readily available to Hg-methylating bacteria in culture (Benoit et al. 2001), and our previous thermodynamic models predict that inorganic Hg-sulfide complexes dominate dissolved Hg speciation under natural sulfidic conditions. However, when we attempted to validate these models in the field, much lower concentrations of neutral dissolved Hg complexes were found than predicted. Laboratory studies revealed a previously unrecognized interaction between Hg, dissolved organic matter (DOM) and sulfide (Miller 2006; Miller et al. 2007). While Hg forms strong complexes with DOM under oxic conditions (Haitzer, et al. 2002; Ravichandran 2004) these complexes had not been expected to form in the presence of sulfide because of the stronger affinity of Hg for sulfide relative to DOM. The observed interaction between Hg and DOM in the presence of sulfide likely involves the formation of a DOM-Hg-sulfide complex, or results from the hydrophobic partitioning of neutral Hg-sulfide complexes into the higher molecular weight DOM (Miller et al. in prep.). However, the structure of these complexes, and their stoichiometry, remain unknown, and therefore cannot be realistically capture in modeling efforts.

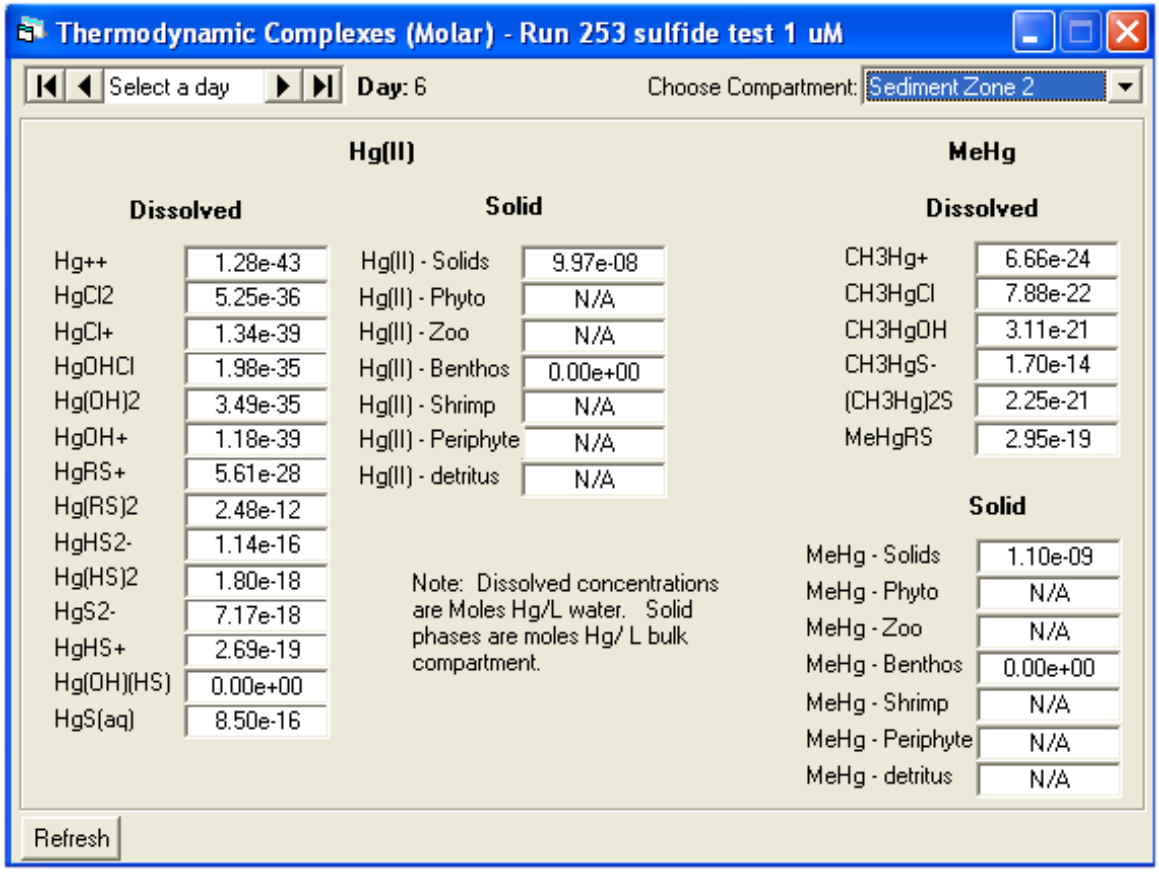

Figure 6.4. Sample E-MCM-predicted Hg complexation with 1 uM total sulfide.

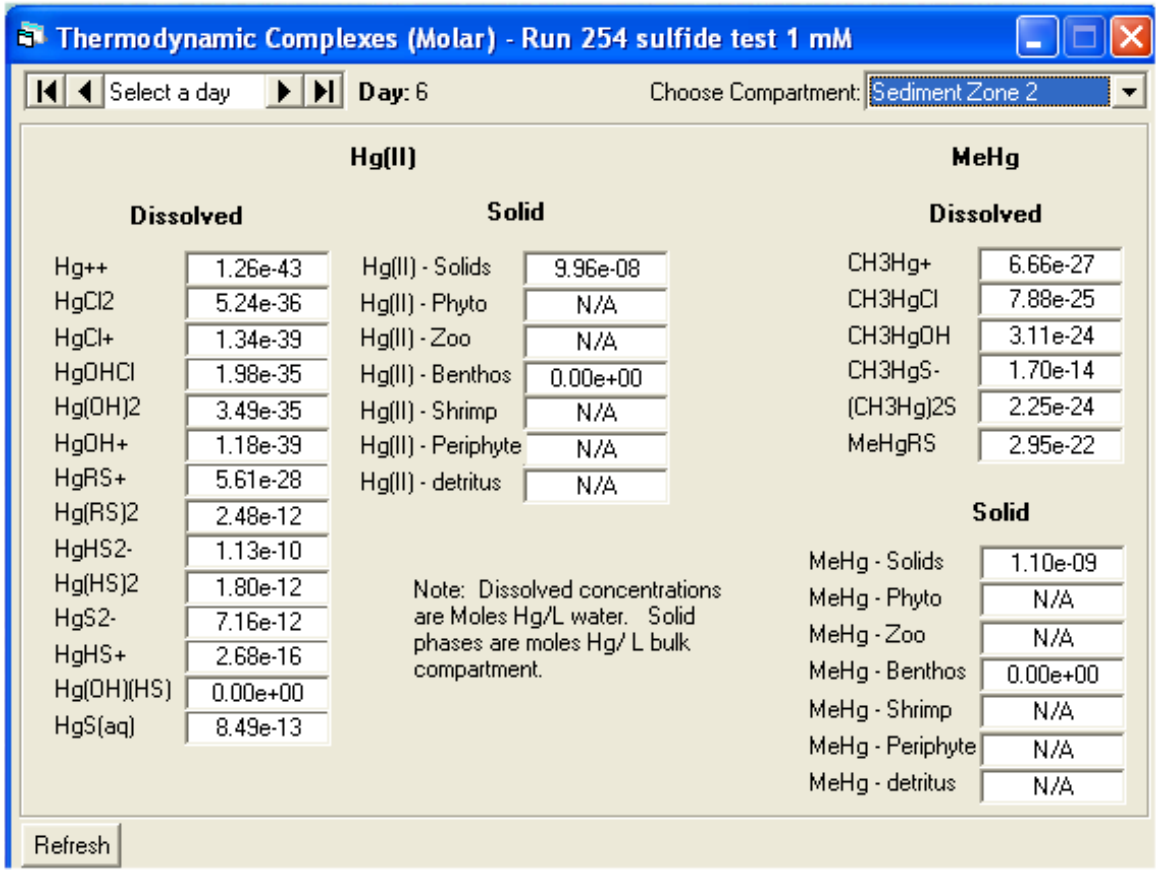

Figure 6.5. Sample E-MCM-predicted Hg complexation with 1 mM total sulfide.

Discussion

Sulfate-dependence

These E-MCM results are generally consistent overall with the hypothesis that sulfate reduction affects methylation and subsequently methylmercury concentrations in Everglades marshes. The model calibration for methylmercury concentrations in water and age 1+ largemouth bass better reflected the extent of observed declines when methylation was linked to sulfate concentration or sulfate reduction rate estimates from the diagenetic model of Roden et al (this study) (Figures 6.3 and 6.4). Model results for young of the year largemouth bass did not improve the results when linking methylation to sulfate (Figure 6.5).

For methylmercury in water or largemouth bass (young of year or age 1+), E-MCM results were similar whether methylation was linked to surface water sulfate concentration or estimates of sulfate reduction rates in sediments (Figures 6.3, 6.4, 6.5). This is not surprising, given that sulfate reduction rates are directly affected by the supply of sulfate at this Everglades site. Large declines in surface water sulfate concentrations at WCA 3A-15 from 1995-2003 resulted in comparable declines in sulfate reduction rates estimates in the diagenetic model of Roden.

The model results suggest that while reductions in sulfate contributed to declines in methylmercury concentrations at WCA 3A-15, other factors also played a role. When methylation was not linked to sulfate, surface water methylmercury and fish mercury concentrations were still predicted to decline between 1995 and 2003. Possible contributing factors include mercury loading rates to the marsh and changes to other water quality conditions. DOC and chloride concentrations declined for example during this period, while pH rose slightly. Wet deposition data from MDN site FP11 were used for the simulations in this study. Longer term monitoring at FP11 (1996- 2006) does not show a systematic decline with time, although there is significant year to year variability (Axelrad et al. 2007). For the specific years simulated here (1995-2003), there was a slight downward trend until 2003 (and afterwards) when wet deposition rates increased. Previous E-MCM hindcasting analyses (Axelrad et al. 2005, C. Pollman unpublished data) suggested that changes in atmospheric deposition during this period were also contributing to declining fish mercury concentrations. Chloride levels also declined at WCA 3A-15 between 1995-2003, ranging from 36 mg L-1 in 1996 to 17 mg L-1 in 1999. In E-MCM, more chloride increases the bioavailability of methylmercury for uptake by phytoplankton, ultimately resulting in higher fish mercury concentration in fish. The decline in chloride during the simulation period was not predicted to influence methylmercury concentrations in water, but did slightly reduce predicted fish mercury concentrations.

While these simulations examine the role of sulfate as a contributing factor to the observed decline in fish mercury concentrations from 1995 to 2003, there could also have been a legacy effect due to conditions prior to 1995, with methylmercury concentrations already declining as of 1995 (even if Hg deposition rates after 1995 had not changed). Further analysis is needed of the relative contributions of changes in sulfate, mercury loading, chloride, DOC and other factors both before 1995 and during the simulation period to the observed decline in fish mercury concentrations.

Sulfide-dependence

Our goal was to develop a mechanistic model of for Hg complexation and bioavailability under the sulfidic conditions found in the more highly sulfur-impacted areas of the EPA. Previous models of Hg-S complexation had not included interactions with DOM, and we attempted to do so here. Through large adjustments of the measured complexation coefficients for Hg with dissolved organic thiols in E-MCM, we were able to fit the model to observed Hg concentration data.

This modeling exercise, coupled with recent laboratory and field data on Hg-D-DOM interactions, suggests that the models being use do not capture one or more important Hg complexes. Work by Miller et al. (2007, in prep) suggests that these are ternary complexes between Hg, sulfide and DOM. In order to make equilibrium complexation models that reflect the inhibition of methylation by sulfide, these complexes will need to be clearly described and their stoichiometry understood.

Thus, while a Hg speciation model that includes both dissolved and solid phase organic matter and sulfides, can be made to adequately predict dissolved Hg concentrations, our existing model is being force fit with a mechanistic understanding of actual complex formation. However, these empirical work-arounds that make it difficult to translate results from one site to another, or to model one location as its biogeochemistry changes through time. Complexation coefficients would need to be recalibrated to each new set

of conditions.

Because significant field data are available to calibrate E-MCM for the higher sulfide areas of the Everglades, an empirically-fit model may be adequate to model the impact of sulfide on MeHg production across the EPA. However, it is obvious that we are missing important complexes in these models, and there are likely to be situations where the model will not function well. More information on Hg-S-DOM complex formation would be needed to do so.

REFERENCES

Atkeson, T.D., D.M. Axelrad, C.D. Pollman, and G.J. Keeler (2003) Integrating Atmospheric Mercury Deposition with Aquatic Cycling in the Florida Everglades: An Approach for Conducting a Total Maximum Daily Load Analysis for an Atmospherically Derived Pollutant. Integrated Summary, Final Report. Prepared by the Florida Department of Environmental Protection, University of Michigan Air Quality Laboratory, and Tetra Tech Inc., 247 pp.

Bates, A. L., E. C. Spiker, and C. W. Holmes. 1998. Speciation and isotopic composition of sedimentary sulfur in the Everglades, Florida, USA. Chemical Geology 146:155-170.Bates, A.L., Orem, W.H., Harvey, J.W., and Spiker, E.C. (2001) Sulfur Geochemistry of the Florida Everglades. U.S. Geological Survey Open-File Report 01-34, 47 p.

Benoit, J. M., Gilmour, C. C., Mason, R. P., Riedel, G. F., Riedel, G. S., and Sullivan, K. 1998. Mercury cycling in the Patuxent River and Estuary, MD, USA. Biogeochemistry 40, 249-265.

Benoit, J.M., C.C. Gilmour, R. P. Mason, and A. Heyes. 1999a. Sulfide controls on mercury speciation and bioavailability in sediment pore waters. Environ. Sci. Technol. 33:951-957.

Benoit, J.M., R. P. Mason and C.C. Gilmour. 1999b. Estimation of mercury-sulfide speciation in sediment pore waters using octanol-water partitioning and implications for availability to methylating bacteria. Environ. Toxicol. Chem. 18:2138-2141.

Benoit, J.M., C.C. Gilmour and R.P. Mason. 2001. Aspects of the bioavailability of mercury for methylation in pure cultures of *Desulfobulbous propionicus* (1pr3). Appl. Environ. Microbiol. 67:51-58.

Benoit, J.M., C.C. Gilmour and R.P. Mason. 2001. The influence of sulfide on solid-phase mercury bioavailability for methylation by pure cultures of *Desulfobulbous propionicus* (1pr3). Environ. Sci. Technol. 35 : 127-132.

Benoit, J.M., R.P. Mason, C.C. Gilmour, and G. R. Aiken. 2001. Constants for mercury binding by dissolved organic carbon isolates from the Florida Everglades. Geochim. Cosmochim. Acta. 65: 4445-4451.

Benoit J. M., Gilmour C. C., Heyes A., Mason R. P., and Miller C. (2003) Geochemical and biological controls over methylmercury production and degradation in aquatic dcosystems. In *Biogeochemistry of Environmentally Important Trace Elements* (ed. Y. Chai and O. C. Braids), pp. 262-297. American Chemical Society. Li Y. and Gregory S. (1974) Diffusion of ions in sea water and in deep-sea sediments. *Geochim. Cosmochim. Acta* **38**, 703-714.

Berg P., Rysgaard S., and Thamdrup B. (2003) Dynamic modeling of early diagenesis and nutrient cycling. A case study in an arctic marine sediment. *Am. J. Sci.* **303**,

905-955.

Berner R. A. (1980) *Early Diagenesis: A Theoretical Approach*. Princeton University Press.

Boudreau B. P. (1996) A numerical-method-of-lines code for carbon and nutrient diagenesis in aquatic sediments. *Comp. Geosci.* **22**, 479-496.

Boudreau B. P. (1997) *Diagenetic Models and Their Implementation*. Springer.

Boudreau B. P., Mucci A., Sundby B., Luther G. W., and Silvergert N. (1998) Comparative diagenesis at three sites on the Canadian continental margin. *J. Mar. Res.* **56**, 1259-1284.

Branfireun, B. A., Roulet, N. T., Kelly, C. A., and Rudd, J. W. M. 1999. *In situ* sulfate stimulation of mercury methylation in a boreal peatland: Toward a link between acid rain and methylmercury contamination in remote environments. Global Biogeochem Cycles.13, 743-750.

Brown P. N., Byrne G. D., and Hindmarsh A. C. (1989) VODE: A variable-coefficient ODE solver. *SIAM J. Sci. Stat. Comput.* **10**, 1038-1051.

Cleckner, L., C.C. Gilmour, D. Krabbenhoft, P. Garrison, and J. Hurley. 1999. Methylmercury production by periphyton in the Florida Everglades. Limnol. Oceanogr. 44:1815-1825.

Compeau, G. C. and R. Bartha. 1985. Sulfate-Reducing Bacteria: Principal methylators of mercury in anoxic estuarine sediment. Appl. Environ. Microbiol. 50:498-502.

Devereux, R., M. R. Winfrey, J. Winfrey, and D. A. Stahl. 1996. Depth profile of sulfate-reducing bacterial ribosomal RNA and mercury methylation in an estuarine sediment. FEMS Microbiol. Ecol. 20:23-31.

Dyrssen, D. and M. Wedborg (1991) The Sulphur-Mercury(H) System In Natural Waters. Water, Air, and Soil Pollution 56:507-519.

Fleming E. J., Mack E. E., Green P. G., and Nelson D. C. (2006) Mercury methylation from unexpected sources: Molybdate-inhibited freshwater sediments and an iron-reducing bacterium. *Appl. Environ. Microbiol.* **72**, 457-464.

Gilmour, C.C., E.A. Henry and R. Mitchell. 1992. Sulfate stimulation of mercury methylation in freshwater sediments. Environ. Sci. Technol. 26:2281-2287.

Gilmour, C.C., G.S. Riedel, M.C. Ederington, J.T. Bell, J.M. Benoit, G.A. Gill and M.C. Stordal. 1998. Methymercury concentrations and production rates across a trophic gradient in the northern Everglades. Biogeochemistry. 40: 327-345.

Haitzer, M, Aiken, GR, and Ryan, JN. 2002. Binding of mercury(II) to dissolved organic matter: the role of the mercury-to-DOM concentration ratio*. Environ Sci Technol*. **36**:3564-3570.

Hsu, H and Sedlak, DL. 2003. Strong Hg(II) complexation in municipal wastewater effluent and surface waters*. Environ Sci Technol*. **37**:2743-2749.

Jensen, S. and A. Jernelov. 1969. Biological Methylation of Mercury in Aquatic Organisms. Nature 223:753. King, J., F. Saunders, R. Lee, and R. Jahnke. 1999. Coupling mercury methylation rates to sulfate reduction rates in marine sediments. Environmental Toxicology and Chemistry 18:1362-1369.

Jeremiason, J. D., Engstrom, D. R., Swain, E. B., Nater, E. A., Johnson, B. M., Almendinger, J. E., Monson, B. A., and Kolka, R. K. 2006. Sulfate Addition Increases Methylmercury Production in an Experimental Wetland. Environ. Sci. Technol. 40(12), 3800-3806.

Kerin E. J., Gilmour C. C., Roden E., Suzuki M. T., Coates J. D., and Mason R. P. (2006) Mercury methylation by dissimilatory iron-reducing bacteria. *Appl. Environ. Microbiol.* **72**, 7919-7921.

King, J. K., J. E. Kostka, M. E. Frischer, and F. M. Saunders. 2000. Sulfate-Reducing Bacteria Methylate Mercury at Variable Rates in Pure Culture and in Marine Sediments . Appl. Environ. Microbiol. 66:2430-2437.

King, J. K., Kostka, J. E., Frischer, M. E., Saunders, F. M., and Jahnke, R. A. 2001. A quantitative relationship that demonstrates mercury methylation rates in marine sediments are based on the community composition and activity of sulfate-reducing bacteria . Environ. Sci. Technol. 35(12): 2491-2496.

Krabbenhoft, D. P., C. C. Gilmour, J. M. Benoit, C. L. Babiarz, A. W. Andren , and J. P. Hurley. 1998. Methylmercury dynamics in littoral sediments of a temperate seepage lake. Canadian Journal of Fisheries and Aquatic Science 55:835-844.

Krabbenhoft, D. P., J. M. Benoit, C. L. Babiarz, J. P. Hurley, and Andren. A.W. 1995. Mercury cycling in the Allequash Creek Watershed, Northern Wisconsin. Water Air and Soil Pollution 80:425-433.

Matisoff G. (1995) Effects of bioturbation on solute and particle transport in sediments. In *Metal contaminated aquatic sediments* (ed. H. E. Allen), pp. 201-272. Ann Arbor Press.

Miller C. L., Mason R. P., Gilmour C. C., and Heyes A. (2007) Influence of dissolved organic matter on the complexation of mercury under sulfidic conditions. *Environmental Toxicology and Chemistry* **26**, 624-633.

Munthe, J., R.A. (Drew) Bodaly, Brian Branfireun, Charles T. Driscoll, Cynthia Gilmour, Reed Harris, Milena Horvat, Marc Lucotte, Olaf Malm. 2007. Recovery of mercury-contaminated fisheries. Ambio. 36: 33-44.

Orem, W.H., H.E. Lerch and P. Rawlik. 1997a. Geochemistry of Surface and Pore Water at USGS 692 Coring Sites in Wetlands of South Florida: 1994 and 1995. U.S. Geological Survey Open- 693 File Report 97-454, pp. 36-39.

Orem, W.H., H.E. Lerch and P. Rawlik. 1997b. Geochemistry of Surface and Pore Water

at USGS Coring Sites in Wetlands of South Florida: 1994 and 1995. U.S. Geological Survey Open-File Report 97-454, pp. 36-39.

Ravichandran, M. 2004. Interactions between mercury and dissolved organic matter - a review*. Chemosphere*. **55**:319-331.

Schiesser W. E. (1991) *The Numerical Method of Lines*. Academic Press.

St. Louis, V. L., J. M. W. Rudd, C. A. Kelly, K. G. Beaty, N. S. Bloom, and R. J. Flett. 1994. The importance of wetlands as sources of methyl mercury to boreal forest ecosystems. Canadian Journal of Fisheries and Aquatic. Science 51:1065-1076.

St. Louis, V. L., J. M. W. Rudd, C. A. Kelly, K. G. Beaty, R. J. Flett, and N. T. Roulet. 1996. Production and loss of methylmercury and loss of total mercury from boreal forest catchments containing different types of wetlands. Environmental Science and Technology 30:2719-2729.

Thamdrup B. and Canfield D. E. (2000) Benthic respiration in aquatic sediments. In *Methods in Ecosystem Science* (ed. O. E. Sala, R. B. Jackson, H. A. Mooney, and R. W. Howarth), pp. 86-103. Springer.

Tetra Tech Inc. 1999b. Dynamic Mercury Cycling Model for Windows 95/NT. A Model for Mercury Cycling in lakes – D-MCM Version 1.0 – User's Guide and Technical Reference. Prepared for EPRI. April 1999.

Tetra Tech Inc. 1999a. Everglades Mercury Cycling Model for Windows 95/NT. A Model for Mercury Cycling in Everglades Marsh Areas – Draft User's Guide and Technical Reference. Version 1.0 Beta. Prepared for the United States Environmental Protection Agency. June 1999.

Tetra Tech (2002) Dynamic Mercury Cycling Model for Windows 98/NT/2000/XP ™ - A Model for Mercury Cycling in Lakes. D-MCM Version 2.0. User's Guide and Technical Reference. November 2002.

Urban et al 1994 Bloom, N., C. Watras, and J. Hurley. 1991. Impact of Acidification on the Methylmercury Cycle of Remote Seepage Lakes. Water Air and Soil Pollution 56:477-491.

VanCappellen P. and Wang Y. (1995) Metal cycling in surface sediments: modeling the interplay of transport and reaction. In *Metal contaminated aquatic sediments* (ed. H. E. Allen), pp. 21-64. Ann Arbor Press.

VanCappellen P. and Wang Y. (1996) Cycling of iron and manganese in surface sediments: a general theory for the coupled transport and reaction of carbon, oxygen, nitrogen, sulfur, iron, and manganese. *Am. J. Sci.* **296**, 197-243.

VanCappellen P., Gaillard J., and Rabouille C. (1993) Biogeochemical transformations in sediments: Kinetic models of early diagenesis. *NATO ASI Series* **1 4**, 401-445.

Westall J. C. (1986) MICROQL I. A chemical equilibrium program in BASIC. *Report 86-*

02, Department of Chemistry, Oregon State University, Corvalis, OR.

Widdel F. and Bak F. (1991) Gram-negative mesophilic sulfate-reducing bacteria. In *The prokaryotes* (ed. H. G. Truper, M. Dworkin, W. Harder, and K.-H. Schleifer), pp. 3352-3378. Springer Verlag.

Wiener, J. G., Knights, B. C., Sandheinrich, M. B., Jeremiason, J. D., Brigham, M. E., Engstrom, D. R., Woodruff, L. G., Cannon, W. F., and Balogh, S. J. Mercury in Soils, Lakes, and Fish in Voyageurs National Park (Minnesota): Importance of Atmospheric Deposition and Ecosystem Factors. Environ. Sci. Technol. 40(20), 6261-6268. 2006.

APPENDIX 1

E-MCM equations for methylation

Three approaches to representing methylation were tested:

a) Methylation is not affected by sulfate.

b) Methylation is related to observed sulfate concentrations.

c) Methylation is related to sulfate reduction rates predicted by the diagenetic model of Roden et al. (this study).

The first two approaches were previously used in E-MCM, and can be represented with equation 1 below. The third approach relating methylation directly to sulfate reduction rates used equation 2 below.

Equation 1: Methylation depends on carbon turnover, available Hg(II) and optionally sulfate concentration.

$$M = (POC_{turnover} + [DOC] \cdot Rd \cdot A \cdot z \cdot p^{i} \cdot (Q_{10m}{}^{(T - Tb) \cdot 0.1})) \cdot k_{meth} \cdot [Hg(II)_{avail}] \cdot (1.0 + (u_{SO4} \cdot [SO_4] / ([SO_4] + K_{so4})))$$

Where:

M = methylation rate (gross rate, not net, μg Hg/day)

$POC^{i}_{turnover}$ = Particulate organic carbon turnover - calculated from mineralization and depends on temperature the carbon fraction in the sediment zone, g POC day^{-1}

[DOC] = DOC concentration in the epilimnetic sediments, g org C/m^2

Rd = DOC decay constant in sediment zone i (day^{-1})

T = temperature in sediment zone i, degrees C

T_b = base temperature at which methylation rate constants apply, degrees C

k_{meth} = methylating efficiency of microbes (ug MeHg ug Hg(II) $avail^{-1}$ (g TOC $m^{-3})^{-1}$)

$[Hg(II)_{avail}]$ = Hg(II) concentration in porewater bioavailable for methylation, ug $Hg(II)/m^3$. (discussed below).

A = area of sediment zone

z = methylation depth in sediment zone, m

p = average porosity of sediment zone, dimensionless

$[SO_4]$ = sulfate concentration in porewater of sediment zone i, μeq L^{-1}

K_{so4} = half-saturation constant for the effect of sulfate on methylation, μeq L^{-1}

u_{SO4} = maximum effect that the presence of sulfate has on the microbial methylation rate.

To eliminate any dependency of methylation on sulfate concentration, K_{so4} is set to zero

Equation 2: Methylation depends on sulfate reduction and available Hg(II)

$$M = SRR \cdot k_{meth} \cdot [Hg(II)_{avail}]$$

Where:

SRR = Sulfate reduction rate (nmoles L^{-1} day^{-1})

k_{meth} = microbial methylating efficiency (ug MeHg ug Hg(II) $avail^{-1}$ (nmole SO_4 $L^{-1})^{-1}$)

For either methylation equation, the user has a choice of 5 options with respect to setting the fraction of dissolved inorganic Hg(II) that can be methylated:

1. free Hg++ ion,
2. $HgCl_2$
3. all non-DOC Hg(II) complexes
4. all dissolved Hg(II), or
5. dissolved neutral Hg(II) species.